

This discussion paper is/has been under review for the journal Biogeosciences (BG).
Please refer to the corresponding final paper in BG if available.

Chemometric perspectives on plankton community responses to natural iron fertilization over and downstream of the Kerguelen Plateau in the Southern Ocean

T. W. Trull^{1,2,3}, D. M. Davies^{1,2}, F. Dehairs⁴, A.-J. Cavagna⁴, M. Lasbleiz⁵,
E. C. Laurenceau^{1,2,3}, F. d'Ovidio⁶, F. Planchon⁷, K. Leblanc⁵, B. Quéguiner⁵,
and S. Blain^{8,9}

¹CSIRO Marine and Atmospheric Research, Hobart, Tasmania, Australia

²Antarctic Climate and Ecosystems Cooperative Research Centre, Hobart, Tasmania, Australia

³Institute for Marine and Antarctic Studies, University of Tasmania, Hobart, Tasmania, Australia

⁴Analytical, Environmental and Geo-Chemistry; Earth Sciences Research Group, Vrije Universiteit Brussel, Belgium

⁵Aix-Marseille Université & Université de Toulon, Marseille, France

⁶LOCEAN – IPSL. Université Pierre et Marie Curie, Paris, France

⁷Laboratoire des Sciences de l'Environnement Marin (LEMAR), Université de Brest, IUEM, France

Chemometric perspectives on plankton community responses to natural iron fertilization

T. W. Trull et al.

Title Page

Abstract

Introduction

Conclusions

References

Tables

Figures

◀

▶

◀

▶

Back

Close

Full Screen / Esc

Printer-friendly Version

Interactive Discussion

⁸Sorbonne Universités, UPMC Univ Paris 06, UMR7621, Laboratoire d'Océanographie Microbienne, Observatoire Océanologique, 66650 Banyuls/mer, France

⁹CNRS, Laboratoire d'Océanographie Microbienne, Observatoire Océanologique, 66650 Banyuls/mer, France

Received: 29 August 2014 – Accepted: 29 August 2014 – Published: 23 September 2014

Correspondence to: T. W. Trull (tom.trull@csiro.au)

Published by Copernicus Publications on behalf of the European Geosciences Union.

BGD

11, 13841–13903, 2014

Chemometric perspectives on plankton community responses to natural iron fertilization

T. W. Trull et al.

Title Page

Abstract

Introduction

Conclusions

References

Tables

Figures

◀

▶

◀

▶

Back

Close

Full Screen / Esc

Printer-friendly Version

Interactive Discussion

Abstract

We examined phytoplankton community responses to natural iron fertilisation at 32 sites over and downstream from the Kerguelen Plateau in the Southern Ocean during the austral spring bloom in October–November 2011. Community structure was estimated from chemical and isotopic measurements (particulate organic carbon POC, ^{13}C -POC, particulate nitrogen PN, ^{15}N -PN, and biogenic silica BSi) on size-fractionated samples from surface waters (300, 210, 50, 20, 5, and 1 μm fractions). Higher values of ^{13}C -POC (vs. co-located ^{13}C -DIC source values) were taken as indicative of faster growth rates, and higher values of ^{15}N -PN (vs. co-located ^{15}N - NO_3 source values) as indicative of greater nitrate use.

Community responses varied in relation to both regional circulation and the advance of the bloom. Iron fertilised waters over the plateau developed dominance by very large diatoms (50–210 μm) with high BSi / POC ratios, high growth rates, and significant ammonium recycling as biomass built up. In contrast, downstream Polar Frontal waters with similar or higher iron supply were dominated by smaller diatoms (20–50 μm) and exhibited greater ammonium recycling. Stations in a deep water bathymetrically trapped recirculation south of the Polar Front with lower iron levels showed the large cell dominance observed on the plateau, but much less biomass. Comparison of these communities to surface water nitrate (and silicate) depletions as a proxy for export shows that the low biomass recirculation feature exported similar amounts of nitrogen to the high biomass blooms over the plateau and north of the Polar Front. This suggests that trophodynamic and export responses differed between regions with persistent low levels vs. punctual high levels of iron fertilisation.

1 Introduction

Natural iron fertilisation from islands, shelves, and plateaus in the Southern ocean produces local and downstream elevations of phytoplankton biomass, ~ 10 -fold higher

BGD

11, 13841–13903, 2014

Chemometric perspectives on plankton community responses to natural iron fertilization

T. W. Trull et al.

Title Page

Abstract

Introduction

Conclusions

References

Tables

Figures

◀

▶

◀

▶

Back

Close

Full Screen / Esc

Printer-friendly Version

Interactive Discussion



Chemometric perspectives on plankton community responses to natural iron fertilization

T. W. Trull et al.

[Title Page](#)[Abstract](#)[Introduction](#)[Conclusions](#)[References](#)[Tables](#)[Figures](#)[⏪](#)[⏩](#)[◀](#)[▶](#)[Back](#)[Close](#)[Full Screen / Esc](#)[Printer-friendly Version](#)[Interactive Discussion](#)

than in surrounding high nutrient low chlorophyll (HNLC) waters, e.g. (de Baar et al., 1995). In some of these systems, carbon export has been observed to be elevated ~ 2–3 fold, e.g. over the Kerguelen Plateau (Blain et al., 2008; Savoye et al., 2008) and to the north of Crozet Island (Pollard et al., 2007). But these studies produced order of magnitude variations in estimates of the amount of carbon export per unit iron supply, as have deliberate iron fertilisation studies (Boyd et al., 2007). These variations appear to reflect both observational limitations and system complexity, including the possibility of variations in initial communities prior to fertilisation (as a result of north-south oceanographic variations or the extent of connection to coastal habitats).

General principles for expected phytoplankton responses have been elucidated, though they remain to be fully tested. These include increased growth rates for all size classes and elevated new production, i.e. increased nitrate use (e.g. Armstrong, 1999; Maldonado et al., 2001). A prevailing view of the overall community response is that it depends on the interaction of these changes with the response of zooplankton grazers, which are thought to be more able to keep up with small cell growth and thus to favour accumulation of larger phytoplankton (Assmy et al., 2013; Morel et al., 1991). This in turn, may favour export, via either direct sinking or aggregation (Smetacek, 1985, 1998). Variations in diatom life cycles and strategies add seasonal complexity to this picture (Queguiner, 2013), and the translation of increases in new production into enhancements in export can be relatively weak (as a result of strong N recycling; Mosseri et al., 2008).

The KEOPS2 expedition sought to examine these and other aspects of community responses to natural iron fertilisation over and downstream of the Kerguelen plateau, in austral spring, October–November 2011, as detailed in the multiple papers in this volume. In this paper, we examine a suite of chemical and isotopic indicators of phytoplankton community structure and function (chemometrics) and relate them to nitrate (and silicate) depletion in surface waters as a proxy for carbon export. The following paragraphs provide an overview of the approach and the structure of the paper.

Chemometric perspectives on plankton community responses to natural iron fertilization

T. W. Trull et al.

[Title Page](#)[Abstract](#)[Introduction](#)[Conclusions](#)[References](#)[Tables](#)[Figures](#)[◀](#)[▶](#)[◀](#)[▶](#)[Back](#)[Close](#)[Full Screen / Esc](#)[Printer-friendly Version](#)[Interactive Discussion](#)

We first describe the complex regional circulation, and use it to cluster the stations into 5 groups (coastal, plateau, waters well downstream near the Polar Front, and waters in a recirculation close to the plateau – separated into an early survey and a later time series). For these groups we briefly summarize the relative levels of iron fertilisation from dissolved and particulate standing stocks (Queroue et al., 2014; van der Merwe et al., 2014) and Fe supply estimates (Bowie et al., 2014; Blain et al., 2014). We also assess the elapsed time since iron fertilisation and its persistence, from seasonal perspectives on vertical mixing (Blain et al., 2014) and Lagrangian perspectives on water mass trajectories around the Kerguelen Plateau (d'Ovidio et al., 2014). We also consider two other overarching perspectives on ecosystem responses: the elapsed time since the beginning of phytoplankton accumulation (from an animation of satellite ocean colour images; Supplement), and the level of biomass enrichment at the time of sampling. Our subsequent chemometric analysis is undertaken at the level of these 5 groups, against this framework of relative intensities and timings of Fe fertilisation and biomass accumulation.

Next, we describe the chemometric approach, i.e. total particulate organic carbon (POC) as an indication of eutrophy, size distribution as a indicator of diversity, biogenic silica/particulate organic carbon (BSi/POC) ratios as a measure of diatom dominance, ^{13}C as a metric for growth rates, and ^{15}N as a metric for ammonium recycling. For our ^{13}C and ^{15}N chemometrics, which present methods to estimate rates from standing stocks, we provide a comparison to shipboard incubation results for growth rates and f ratios (from ^{13}C and ^{15}N tracer uptake experiments, Cavagna et al., 2014). To determine nitrate (and silicic acid) depletion by the biological pump, we explore both temperature and salinity based approaches to estimate initial winter surface water concentrations, and also evaluate the fraction of the observed depletion that still remains in the water column for potential future export (using particulate nitrogen and biogenic silica stocks from CTD casts; Lasbleiz et al., 2014; Blain et al., 2014).

Finally, with help from additional comparisons to ^{234}Th depletions (Planchon et al., 2014) and sediment trap collections (Laurenceau et al., 2014), we arrive at an overview

of the relative importance of Fe inputs and temporal evolution in the control of community structure and carbon export.

2 Methods

2.1 Site description

5 The KEOPS2 campaign was carried out in October–November 2011 over and downstream of the Kerguelen Plateau in the Southern Ocean, under conditions of complex circulation and rapidly changing phytoplankton biomass, as summarized in Figs. 1 and 2, and further showcased in the full annual satellite chlorophyll animation (Supplement).

10 The Kerguelen Plateau is a northwest-southeast oriented seafloor feature which rises to ~ 500 m below the surface over much of its extent. It also hosts several volcanic islands, in particular the large Kerguelen Island archipelago in the north and the smaller Heard Island at the southern edge of the central Kerguelen Plateau. The plateau blocks the eastward flowing Antarctic Circumpolar Current (ACC). Much of the ACC flow goes to the south of the plateau and through the Fawn Trough (to the south of Heard Island), with a smaller portion associated with the Subantarctic Front flowing around the northern edge of Kerguelen Island. A narrow jet of ACC water also flows across the plateau in the narrow, mid-depth (~ 1000 m) channel just to the south of Kerguelen Island (Fig. 1). This feature corresponds with the northernmost presence of a subsurface temperature minimum formed by winter cooling (near 200 m depth), and thus defines the northernmost branch of the Polar Front (Park et al., 2008, 2014b; d'Ovidio et al., 2014). This jet was a particularly important feature of the area sampled during KEOPS2, because it separated the central plateau and downstream offshore stations to the south of the Polar Front (PF), from those to the north of the PF, where the coastal stations were also located. As discussed in Sect. 2.2, the modes of supply of Fe to the waters north and south of this jet may also differ, with some downstream

Polar Front stations potentially influenced by Fe inputs from coastal waters associated with Kerguelen Island or its shallow northern shelf (Blain et al., 2014).

From a dynamical perspective, the full ocean depth branch of the Polar Front lies to the south of Heard Island, where the ACC flow transits the Fawn Trough (Sokolov and Rintoul, 2009). As this flow passes to the east of the plateau it follows the bathymetric contours to the north where it enters a bathymetrically-trapped recirculation region to the south of the Polar Front, before eventually exiting downstream (Park et al., 2008, 2014b; d'Ovidio et al., 2014). This recirculation feature and the flow along the PF jet are fixed in space by the bathymetry close to the plateau, but at their eastern edge over the abyssal plain (where the strong ACC flows passing south and north of the plateau re-join) meandering is strong and varies with time. For example, the animation of ocean colour (Supplement) suggests the PF moved southward in this region over the course of the KEOPS2 observations.

As shown in Fig. 1, the initial sampling was carried out along a deep water transect (stations TNS 1–10) run northwards from the central plateau (TNS-10) across the recirculation feature and Polar Front and into Subantarctic waters (TNS-1). This was followed by a west to east transect (stations TEW 1–8) running offshore from the Kerguelen Island coast, across the middle of the recirculation, and reaching the southward meandering Polar Front in the far east of the study region. This initial survey was followed by multiple “time-series” visits to the recirculation feature, (designated as stations E1–E5, with two stations at the E4 time step – to the western side, E4-W, and eastern side, E4-E, of this recirculation). In addition several other features at the margins of the survey region were also sampled, with rather complicated nomenclature based on locations, links to other programs, durations, and purposes:

- reference HNLC waters to the west of the plateau (stations R and R2).
- A central plateau station that had served as the bloom reference site in the previous KEOPS campaign in late summer/autumn 2005 (station A3).

BGD

11, 13841–13903, 2014

Chemometric perspectives on plankton community responses to natural iron fertilization

T. W. Trull et al.

Title Page

Abstract

Introduction

Conclusions

References

Tables

Figures

◀

▶

◀

▶

Back

Close

Full Screen / Esc

Printer-friendly Version

Interactive Discussion

Chemometric perspectives on plankton community responses to natural iron fertilization

T. W. Trull et al.

[Title Page](#)

[Abstract](#)

[Introduction](#)

[Conclusions](#)

[References](#)

[Tables](#)

[Figures](#)

[◀](#)

[▶](#)

[◀](#)

[▶](#)

[Back](#)

[Close](#)

[Full Screen / Esc](#)

[Printer-friendly Version](#)

[Interactive Discussion](#)

- High biomass waters in the extreme northeast of the study region, near the downstream location of the Polar Front (Stations F-L and F-S; L for long, S for short).
- Two stations carried out to compare geochemical tracer concentrations in waters over the plateau (G1) with Kerguelen coastal waters (G2).

All of these stations (except TNS-4 and TNS-7) on the initial survey transect were sampled for our size-fractionated chemometric analyses (with some stations also sampled both at night and day).

The five colour-coded Groups mapped in Fig. 1 cluster the KEOPS2 stations based largely on the interactions of the circulation with the bathymetry (with some additional regard for temporal evolution and the timing and extent of iron supply and biomass accumulation, as discussed below). The properties of these Groups are summarized in Table 1. In brief, Groups 1 and 2 cluster stations from the recirculation feature. Group 1 consists of stations in this region occupied during the initial transects when biomass was low, and also for convenience includes the upstream HNLC reference site R2. Group 2 holds the stations occupied as a pseudo-Lagrangian time series within the recirculation. Group 3 holds the central plateau stations, including waters that flow northward to leave the plateau along the south side of the Polar Front jet. Group 4 has the coastal stations; although the inclusion of TEW-3 is debateable given its location at the plateau edge. Group 5 has the downstream stations near and north of the Polar Front. Two stations in this Group, at the northern Subantarctic end of the initial survey, TNS-1 and TNS-2, were included to keep the number of Groups low, but stand out as quite distinct in having lower biomass with greater proportions of non-diatom taxa (Lasbleiz et al., 2014). Additional discussion of stations near the boundaries of these Groups is provided below, and other clusterings are possible, especially for stations at the boundaries among the Groups (for further discussion see Lasbleiz et al., 2014).

The majority of the analysis presented in this paper is based on comparisons across these Groups rather than individual stations (although variations within the Groups do

occur and sometimes provide additional insights, and for this reason the figures display the individual stations in each group in chronological order (e.g. see Fig. 3).

2.2 Intensity and timing of Fe fertilisation

Iron sampling and analysis was carried out at a much-reduced subset of the stations discussed here, albeit with greater vertical resolution (Bowie et al., 2014; van der Merwe et al., 2014; Queroue et al., 2014). Thus, comparisons to our results are only possible at the level of our station Groups, and only in a relative sense. The lowest Fe levels were observed at the HNLC reference station upstream to the west of the Kerguelen Plateau (slightly less than 0.1 nM at station R2). The recirculation region (Groups 1 and 2) had low to moderate dissolved Fe (0.06–0.38 nM at stations E2, E3 and E5). Slightly higher minimum concentrations were observed over the plateau (0.18–0.21 nM at the Group 3 stations A3-1 and G1). Moderate enrichments were also observed in the Group 5 downstream waters near the Polar Front (~ 0.26 nM at station F-L). The highest dissolved Fe levels were in the Group 4 Kerguelen Island coastal waters (surface concentrations of 2.17 nM for TEW 1 and 1.26 nM for TEW 2).

Particulate Fe levels were not measured in coastal waters, but generally exceeded dissolved Fe levels in the Group 3 stations over the plateau (by factors of 13–20) and offshore in the Group 1 and 2 stations in the recirculation feature and the single Group 5 station in the downstream plume (by factors of 2–34). The bio-availability of this particulate Fe is unknown, but assuming a conservative fraction of 1 % (for discussion see van der Merwe et al., 2014) leads to a 20 % increase over the plateau of available iron and 4–34 % increase offshore.

Estimating Fe supply is more difficult. It appears possible that downstream waters north of the Polar Front (Group 5 stations F-S, F-L, TEW-7, and TEW-8, but not the Subantarctic influenced stations TNS-1 and TNS-2) receives more iron than the plateau (Group 3) especially in summer when stratification reduces vertical supply over the plateau, but advection continues to sweep iron-rich coastal waters from the northern

BGD

11, 13841–13903, 2014

Chemometric perspectives on plankton community responses to natural iron fertilization

T. W. Trull et al.

Title Page

Abstract

Introduction

Conclusions

References

Tables

Figures

◀

▶

◀

▶

Back

Close

Full Screen / Esc

Printer-friendly Version

Interactive Discussion

Kerguelen shelf along the northern side of the Polar Front jet (Blain et al., 2014; Bowie et al., 2014).

The nature of Fe fertilisation also varies among the regions, in terms of both its timing relative to our sampling, and its persistence. Recent and brief iron fertilisation appears likely to characterize the Polar Front (Group 5 region). Water parcel trajectories calculated from drifter trajectories and altimetry based geostrophic currents (d'Ovidio et al., 2014) suggest times of less than 0.5 to 1 month for the downstream Polar Front stations (Group 5 stations F-S, F-L, TEW-7, TEW-8), with rapid dispersal and thus low persistence. In comparison, it appears to take longer for northern Kerguelen shelf waters to reach the recirculation region (Group 1 and 2 stations), where the water is then retained for a relatively long time, but is also diluted by approximately equal volumes of waters derived from the south (D'Ovidio et al., 2014; Park et al., 2014a). These supply paths are also indicated by Ra isotope distributions (Sanial et al., 2014). Thus fertilisation of the recirculation feature appears to be less recent and intense than that of the Polar Frontal region, but probably more persistent. For the Kerguelen coastal stations (Group 4), where water columns were well mixed to the bottom, fertilisation is both recent and persistent. Fertilisation over the plateau is also relatively recent in a seasonal context, having presumably reached a maximum at the time of deepest winter mixing (i.e. ~ 2 months from maximum cooling in August–September to sampling in October–November and) and continued episodically via entrainment through spring. Its persistence may be similar or somewhat larger than that of the recirculation region given estimates of water parcel residence times over the plateau of order 2–3 months (Park et al., 2008).

In summary, this evaluation of iron inputs yields rank orders as follows:

Intensity of Fe fertilisation (lowest to highest):

recirculation feature < *plateau* < \approx *Polar Front plume* \ll *coastal stations*

Elapsed time since Fe fertilisation and its persistence (most recent to oldest):

Polar Front plume < *recirculation feature* < \approx *plateau* < *coastal stations*

Chemometric perspectives on plankton community responses to natural iron fertilization

T. W. Trull et al.

Title Page

Abstract

Introduction

Conclusions

References

Tables

Figures

◀

▶

◀

▶

Back

Close

Full Screen / Esc

Printer-friendly Version

Interactive Discussion



For easy reference these properties are summarized for the station Groups in Table 1.

2.3 Intensity and timing of phytoplankton biomass accumulation

The KEOPS2 sampling was carried out in spring, spanning the period when phytoplankton biomass was rapidly increasing both over and downstream of the plateau, forming rather complex patterns in satellite chlorophyll images (Fig. 2). Thus the time of sampling relative to the development of surface biomass enrichment varied strongly among the stations. The sequence of ocean colour images in Fig. 2. (see also the Supplement) suggests that this occurred first in coastal Kerguelen Island waters (starting in mid-September very close to the island and extending northwards by mid October; but reaching only moderate Chl *a* levels near $1 \mu\text{g L}^{-1}$), followed by the downstream plume north of the Polar Front (near Group 5 stations F-S, F-L, TEW-7, TEW-8) where chlorophyll biomass jumped very rapidly from below 0.5 to above $2 \mu\text{g L}^{-1}$ early in the first week of November.

At this time (as shown in the animation in the Supplement), the central plateau and the recirculation feature still had only minor biomass development, with concentrations near $0.5 \mu\text{g L}^{-1}$. But, within a few days, by 9 November, all strongly Fe enriched regions (coastal, central plateau, and the downstream waters near the Polar Front) had Chl *a* levels above $2.5 \mu\text{g L}^{-1}$. Yet, the recirculation region still had low levels of $\sim 0.5 \mu\text{g L}^{-1}$ for another week, and only reached levels of $1\text{--}1.5 \mu\text{g L}^{-1}$ by end November. Only in early December, after the end of field sampling, did the recirculation feature reach levels of $2.5\text{--}3 \mu\text{g L}^{-1}$. Interestingly, the downstream waters near the Polar Front maintained high levels throughout most of this period, but the central plateau bloom faded (as sampled by station A3-2) before being replaced by a second bloom somewhat further east, though still over the plateau. The animation of these satellite chlorophyll images provides further detail of the structure and sequence of biomass accumulation, both during and after the voyage (Supplement).

In summary, satellite biomass accumulation yields rank orders as follows:

13851

Chemometric perspectives on plankton community responses to natural iron fertilization

T. W. Trull et al.

Title Page

Abstract

Introduction

Conclusions

References

Tables

Figures

◀

▶

◀

▶

Back

Close

Full Screen / Esc

Printer-friendly Version

Interactive Discussion



Chemometric perspectives on plankton community responses to natural iron fertilization

T. W. Trull et al.

[Title Page](#)[Abstract](#)[Introduction](#)[Conclusions](#)[References](#)[Tables](#)[Figures](#)[⏪](#)[⏩](#)[◀](#)[▶](#)[Back](#)[Close](#)[Full Screen / Esc](#)[Printer-friendly Version](#)[Interactive Discussion](#)

zooplankton have shorter life cycles). Thus our primary chemometric tool is to simply examine variations in the distribution of POC across the size fractions as an indicator of community structure. (To remove the influence of our particular choice of filter sizes, we express the POC concentration variations as spectra, i.e. we divide the concentrations by the width of each filtration interval, yielding units of $\mu\text{M } \mu\text{m}^{-1}$). Secondly we use high BSi/POC ratios as an indication of community dominance by diatoms (of course this is simplistic given the presence of silicoflagellates at some stations (Lasbleiz et al., 2014) and the occurrence of a wide range of BSi/POC ratios in diatoms (Ragueneau et al., 2006), and low POC/PN ratios as an indication of contributions from heterotrophic biomass (below the values of ~ 6 – 7 that characterise most phytoplankton; e.g. Anderson and Sarmiento, 1994; Redfield et al., 1963).

2.5.1 Isotopic chemometric principles – ^{13}C

The isotopic chemometric tools are not as common and require greater explanation. Variations in ^{13}C -POC and ^{15}N -PN values derive from both primary photosynthetic production and the overlay of secondary heterotrophic imprints, especially in the smallest size fraction (1–5 μm) in which bacterial processing was important and the two largest size fractions (210–300 and 300–1000 μm) which contained significant contributions from zooplankton. For the middle size fractions (5–20, 20–50 and 50–210 μm), biomass was dominated by phytoplankton and thus these fractions can be used to examine the impacts of iron fertilisation and other controls on primary production. This is our focus for the use of these tools. In particular we interpret ^{13}C enrichment as indicative of higher growth rates and ^{15}N enrichment as indicative of higher f ratios (i.e. greater use of nitrate in comparison to reduced forms of nitrogen). In the following paragraphs we introduce quantitative expressions for these relationships, but also acknowledge that they rest on many assumptions, which we evaluate further in light of our results. After this discussion of these autotrophic expressions, we also briefly describe the scale of heterotrophic effects.

Chemometric perspectives on plankton community responses to natural iron fertilization

T. W. Trull et al.

[Title Page](#)

[Abstract](#)

[Introduction](#)

[Conclusions](#)

[References](#)

[Tables](#)

[Figures](#)

[⏪](#)

[⏩](#)

[◀](#)

[▶](#)

[Back](#)

[Close](#)

[Full Screen / Esc](#)

[Printer-friendly Version](#)

[Interactive Discussion](#)



Controls on the ^{13}C composition of phytoplankton are complex (Goericke et al., 1994), but in general, within a phytoplankton size-class (and relative to source compositions) ^{13}C enrichment is a sign of faster growth (Popp et al., 1998, 1999; Rau et al., 1997; Trull et al., 2008). In other words, discrimination against ^{13}C assimilation is less strong in rapidly growing cells. We briefly review the processes involved in this discrimination to inform our use of ^{13}C -POC variations to estimate approximate growth rates, and return to this issue again in the results section in light of the specifics of the KEOPS2 observations.

One possible control is a change from use of the scarce molecular CO_2 form of DIC to greater use of the ~ 100 -fold more abundant bicarbonate form (although this form is electrically charged and thus likely to be more energetically costly to assimilate). Assimilation of bicarbonate raises ^{13}C -POC, because it has much higher ^{13}C contents than dissolved molecular CO_2 ($\sim 11\%$ higher at KEOPS2 temperatures, as expressed by the approximate equilibrium fractionation expression; Rau et al., 1997):

$$^{13}\text{C}\text{-CO}_2 = ^{13}\text{C}\text{-DIC} + 23.644 - 9701.5/T_{\text{kelvin}} \quad (1)$$

There is presently no understanding of how a possible switch from CO_2 to HCO_3^- assimilation might depend on growth rate, but some aspect of the relative availability of CO_2 supply vs. biological demand is likely to be involved. This balance also affects the extent of fractionation that occurs if only one external species (e.g. molecular CO_2) is assimilated, and models of supply vs. demand have been shown to reproduce ^{13}C variations well for many phytoplankton (e.g. Rau et al., 1997; Popp et al., 1998), and we rely on this approach to re-express our field ^{13}C variations in terms of (relative) growth rates.

The discrimination against ^{13}C that accompanies intra-cellular enzymatic fixation of CO_2 ($\epsilon_f \sim 25\text{--}28\%$ for the most common enzymes but less for other forms) exceeds the isotopic offset between the external DIC species, and thus has been a focus for the likely control on fractionation during carbon assimilation. The extent to which this enzymatic discrimination is expressed in the ^{13}C -POC depends on the balance of sup-

Chemometric perspectives on plankton community responses to natural iron fertilization

T. W. Trull et al.

[Title Page](#)

[Abstract](#)

[Introduction](#)

[Conclusions](#)

[References](#)

[Tables](#)

[Figures](#)

[◀](#)

[▶](#)

[◀](#)

[▶](#)

[Back](#)

[Close](#)

[Full Screen / Esc](#)

[Printer-friendly Version](#)

[Interactive Discussion](#)

ply into the cell vs. demand from growth. If all supply is assimilated ^{13}C -POC equals the supply value, but if little is assimilated (with the rest re-exported), the full enzymatic fractionation occurs (i.e. ^{13}C -POC approaches the supply value minus ε_f). Laboratory experiments have confirmed the general validity of the supply vs. demand model and shown (for a limited set of phytoplankton) that ^{13}C -POC increases linearly with growth rate (Popp et al., 1998). Specifically, Popp et al. (1998) applied the model that:

$$^{13}\text{C}\text{-POC} = (^{13}\text{C}_{\text{source}} - \varepsilon_f) + k \text{ demand-rate/supply-rate} \quad (2)$$

in which the first term expresses the lowest possible ^{13}C contents of the cell as growth rate approaches zero, and the second term describes the linear (constant k) dependence of isotopic composition on the relative rates of CO_2 supply into the cell and its cellular fixation. They found an excellent fit to data by assuming the chemical form is aqueous molecular CO_2 and that supply rate depends linearly on its external concentration modulated by the surface to volume ratio (S/V) of the cell:

$$^{13}\text{C}\text{-POC} = (^{13}\text{C}\text{-CO}_2 - 25) + 182 \mu / ([\text{CO}_2]S/V) \quad (3)$$

Rewriting this equation for growth rate, μ , and our measured ^{13}C -DIC and ^{13}C -POC values yields a possible path to quantitative growth rates for our size fractions:

$$\mu = S/V[\text{CO}_2][^{13}\text{C}\text{-POC} - (^{13}\text{C}\text{-CO}_2 - 25)]/182 \quad (4)$$

with $^{13}\text{C}\text{-CO}_2$ calculated using Eq. (1), $[\text{CO}_2]$ obtained from underway $p\text{CO}_2$ observations (Lo Monaco et al., 2014) and Henry's Law (Weiss, 1974). In this expression, growth rate μ is in d^{-1} , S/V in μm^{-1} , and $[\text{CO}_2]$ in $\mu\text{mol kg}^{-1}$.

As discussed further in the results section, this expression predicts two useful things. Firstly, it predicts growth rates that we compare to other estimates. Secondly it shows that a given ^{13}C -POC increase predicts a larger increase in growth rate for small cells than for large cells, because smaller cells have higher S/V (and this sensitivity to S/V

is large). Of course, comparison of these rates is sensitive to S/V estimates and to the assumption that transport into and out of the cell scales with this parameter. For this reason, our growth rate estimates must be viewed with great caution.

Trophic ^{13}C enrichment is thought to be relatively small within a given class of compounds for carbon ($\sim 1\%$ per trophic level; Michener and Schell, 1994). However, accumulation of lipids, which are ^{13}C depleted owing to their multi-step synthesis pathways, causes many zooplankton to have lower ^{13}C contents than their diet (Michener and Schell, 1994; Syvaranta and Rautio, 2010). This is a probable contributor to the ^{13}C -POC values of the two largest size fractions, as discussed in the results section.

Finally, because our focus is on extracting information about growth conditions for the communities at the time of sampling, we remove the influence of source inorganic carbon isotopic composition spatial variations on the ^{13}C -POC variations, by considering only their offset relative to the source rs: $^{13}\text{C-POC}_{rs} = ^{13}\text{C-POC} - ^{13}\text{C-DIC}$.

2.5.2 Isotopic chemometric principles – ^{15}N

Phytoplankton ^{15}N -PN variations result primarily from the relative use of reduced nitrogen (mainly ammonium) which has low ^{15}N contents vs. the more abundant nitrate pool which has higher ^{15}N contents, and secondarily from variations in the isotopic fractionation accompanying nitrate assimilation (Goericke et al., 1994; Karsh et al., 2003, 2014; Trull et al., 2008). As with the carbon isotopes, we discuss the ^{15}N -PN variations relative to co-located $^{15}\text{N-NO}_3$ source values ($^{15}\text{N-PN}_{rs} = ^{15}\text{N-PN} - ^{15}\text{N-NO}_3$), to separate source composition effects (that have accumulated from the history of nitrogen metabolism in a given parcel of water) from the fractionation associated with current PN production. This source composition effect was larger for nitrogen than for carbon, because variation in $^{15}\text{N-NO}_3$ values was larger (6.1–8.‰), and $^{15}\text{N-PN}$ variations were smaller (6‰).

By estimating expected values for $^{15}\text{N-PN}_{rs}$ formation from nitrate and from ammonium, estimates of new vs. recycled production (i.e. f ratios) can be obtained for each size fraction by mass balance. The observed range of fractionation factors for nitrate

assimilation during KEOPS2, (ϵ_{na} of -4 to -4.5% , as estimated from $^{15}\text{N-NO}_3$ variations in the water column; Dehairs et al., 2014) provides an upper limit for growth on nitrate of $^{15}\text{N-PN}_{rs}$ (-4%). For ammonium, the simplest approximation is to use a value just below the lowest observed $^{15}\text{N-PN}_{rs}$, i.e. to assume that these cells grew on ammonium alone (Trull et al., 2008). Using these end members ($^{15}\text{N-PN}_{Nrs} = -4\%$ for growth on nitrate; $^{15}\text{N-PN}_{Ars} = -8\%$ for growth on ammonium), yields f ratio estimates for each size-fraction, from:

$$f = ({}^{15}\text{N-PN}_{rs} - {}^{15}\text{N-PN}_{Ars}) / ({}^{15}\text{N-PN}_{Nrs} - {}^{15}\text{N-PN}_{Ars}) \quad (5)$$

In comparison to carbon, trophic enrichment of ^{15}N is relatively large (3% vs. $\sim 1\%$; (Michener and Schell, 1994; Wada and Hattori, 1978), which provides a cautionary note on the interpretation of the f ratio estimates. The largest zoo-plankton containing size fractions ($210\text{--}300\ \mu\text{m}$, $300\text{--}1000\ \mu\text{m}$) have higher $^{15}\text{N-PN}_{rs}$ values than are achievable by primary production and derive from this process.

3 Results

3.1 Total biomass variations

POC biomass concentrations in surface waters varied from ~ 3 to $25\ \mu\text{M}$ (Table 2), reported as the “total” sum of fractions as filtered from as much as $2600\ \text{L}$ of underway supply water, and are in agreement with our $1\ \text{L}$ single filter “bulk” filtrations (Appendix A). Although there are some differences in POC results across the multiple sample methodologies of the entire mission e.g. underway supply, Niskin bottles, in-situ pumps (Tremblay et al., 2014; Dehairs et al., 2014; Lasbleiz et al., 2014) these remain to be fully assessed hence we focus on our own internally consistent results.

There were significant variations of POC concentrations within the Groups as well as among them (Fig. 3). The Group 1 upstream Fe-poor HNLC reference station R2

Chemometric perspectives on plankton community responses to natural iron fertilization

T. W. Trull et al.

Title Page

Abstract

Introduction

Conclusions

References

Tables

Figures

◀

▶

◀

▶

Back

Close

Full Screen / Esc

Printer-friendly Version

Interactive Discussion



Chemometric perspectives on plankton community responses to natural iron fertilization

T. W. Trull et al.

[Title Page](#)[Abstract](#)[Introduction](#)[Conclusions](#)[References](#)[Tables](#)[Figures](#)[◀](#)[▶](#)[◀](#)[▶](#)[Back](#)[Close](#)[Full Screen / Esc](#)[Printer-friendly Version](#)[Interactive Discussion](#)

and the early sampled furthest south and coldest Group 3 plateau station A3–1 had the lowest values. The recirculation initial survey Group 1 had somewhat higher values (5–10 μM ; with a single higher value of 15 at TEW-4), with little increase over time as represented by the Group 2 recirculation time series (again with a single outlier at E4-E). The Group 5 downstream Polar Front bloom stations had the highest biomasses, exceeding all but 1 of the Group 3 Plateau stations as well as all Group 4 coastal stations. Note that the Group 5 stations from warmer waters north of and near the Subantarctic front (TNS 1 and 2), where the upstream flow may not cross the Kerguelen shelf, stand out from the other Group 5 stations as having much lower biomass, similar to the upstream HNLC reference station (R2). This distribution of POC among the Groups provides important results: (i) waters that have not crossed the plateau have low biomass, presumably reflecting a lack of Fe fertilisation, and (ii) downstream blooms achieve higher concentrations of biomass than coastal blooms. Given that Fe concentrations were highest in the coastal waters (Table 1; Sect. 2.2), this means that ecosystem dynamics must also contribute importantly to the control of biomass.

Distributions of POC with particle size also varied significantly (Fig. 3). All stations exhibited the highest concentrations in the smallest size fraction (1–5 μm) *when normalized to the width of this fraction interval* (Fig. 3), but these concentrations were relatively constant across the Groups. In contrast the concentrations in the three phytoplankton dominated intermediate size fractions (5, 20, 50 μm filters) varied among the groups, and drove the total POC biomass changes described above. There were significant variations within these 3 size fractions as well. Abundance decreased monotonically with size at the HNLC reference station. The Group 1, and even more so the Group 2, stations exhibited greater increases (as total biomass increased either among stations in Group 1 or with time in the Group 2 time series; note that Table 2 lists all stations in chronological order) in the 20 μm fraction than the 5 μm fraction, but still low values in the 50 μm fraction. The Group 3 plateau stations started with this slightly “humped” (i.e. $5 < 20 > 50 \mu\text{m}$) POC distribution, but as biomass increased the 50 μm fraction came to dominate. Interestingly, this never occurred in the Group 4 coastal or

Group 5 Polar Frontal biomass rich stations, which remained dominated by the 20 μm size fraction.

Heterotrophic biomass (as represented by the two largest size filters, 210 and 300 μm) was generally an order of magnitude lower than autotrophic biomass (as represented by the 3 intermediate fractions), and more than 2 orders of magnitude lower if the smallest fraction is also included. It generally increased with total biomass in all the Groups, except the Group 4 coastal waters. Station TEW-4 in Group 1 had unusually high heterotrophic biomass, which explains its outlier status of exceptionally high total POC for this Group.

3.2 Variations in BSi concentrations and associated contributions to biomass

BSi estimates were not possible for the smallest size fraction (owing to use of a quartz 1 μm filter). Thus total BSi is underestimated, and comparisons to total POC must be done cautiously. As shown in Fig. 3 (top row), the highest BSi levels were observed in the Plateau stations late in the voyage, with these exceeding those of the Group 5 Polar Frontal bloom stations as well as all the other Groups. The lowest levels were in the Polar Frontal Zone and Subantarctic stations (Group 5, stations TNS1 and 2). More detailed evaluation is possible on a size-fractionated basis. The initial survey of Group 1 low biomass waters found a wide range of BSi/POC ratios that covered most of the variability seen across the entire KEOPS2 study (Fig. 3; bottom row). Among the other groups, the Group 3 plateau stations stands out for having high BSi/POC ratios in all the autotrophic fractions (5, 20, 50 μm filters), in contrast to uniformly low ratios for the Group 5 stations. The presence of non-zero BSi/POC ratios in many of the largest, zooplankton dominated size fractions (210 and 300 μm filters) reflects the presence of chain-forming diatoms, although their POC biomass was insignificant in comparison to that of the autotrophic intermediate fractions.

Much of the range in BSi/POC ratios for the intermediate size fractions overlaps with that expected for diatoms under iron-impoverished (BSi/POC \sim 0.6) to iron-replete (BSi/POC \sim 0.15) conditions (Hoffman et al., 2007; Hutchins and Bruland, 1998;

Chemometric perspectives on plankton community responses to natural iron fertilization

T. W. Trull et al.

Title Page

Abstract

Introduction

Conclusions

References

Tables

Figures

⏪

⏩

◀

▶

Back

Close

Full Screen / Esc

Printer-friendly Version

Interactive Discussion



Takeda, 1998), but note that this is a simplistic view of diatom BSi/POC variations in response to Fe inputs which ignores variations across taxa and across life cycle stages (Leynaert et al., 2004; Marchetti and Cassar, 2009; Ragueneau et al., 2006; Hoffman et al., 2007). There was no clear correspondence across the groups between BSi/POC values and Fe fertilisation levels, in that the Group 4 Fe-rich coastal waters had intermediate BSi/POC ratios in comparison to the moderately Fe-rich Group 3 plateau and Group 5 downstream Polar Front waters. Community variations in the ratio of diatom to non-diatom taxa thus appear to overprint any dependence on Fe for diatom BSi/POC ratios.

3.3 ^{13}C variations

We first note that the $^{13}\text{C}\text{-POC}_{\text{rs}}$ values of the HNLC reference station (R-2) were the lowest of all stations, and we take them as an indication of expectations for slowly growing offshore polar phytoplankton (Fig. 4). In comparison, Group-1 and Group-2 stations (which had indistinguishable $^{13}\text{C}\text{-POC}_{\text{rs}}$ values), were elevated by $\sim 2\text{‰}$ (ranging from 1 to 4 ‰) in comparison to the R-2 HNLC reference level. These stations also displayed an increase in $^{13}\text{C}\text{-POC}_{\text{rs}}$ values from the smallest (1–5 μm) towards larger size fractions (5–20, 20–50 μm) before decreasing again in the largest autotrophic size fraction (50–210 μm) and generally also in the heterotrophic dominated size fractions (210–300 and 300–1000 μm). This hump-shaped pattern was also present at the Group-3 plateau stations, where $^{13}\text{C}\text{-POC}_{\text{rs}}$ values were elevated further. The Group-4 coastal stations had the highest $^{13}\text{C}\text{-POC}_{\text{rs}}$ values, with values as high as -20‰ .

This pattern has been found before in Antarctic polar waters, with the initial increase in $^{13}\text{C}\text{-POC}_{\text{rs}}$ with size attributed to the effect of decreasing surface/volume on CO_2 uptake (Popp et al., 1998, 1999), and the subsequent decrease in larger fractions attributed to the presence of needle-shaped diatoms with high surface/volume (S/V) ratios similar to small cells (Trull and Armand, 2001). Detailed S/V estimates for our samples are not yet available to assess this explanation or the influence of the pres-

BGD

11, 13841–13903, 2014

Chemometric perspectives on plankton community responses to natural iron fertilization

T. W. Trull et al.

Title Page

Abstract

Introduction

Conclusions

References

Tables

Figures

◀

▶

◀

▶

Back

Close

Full Screen / Esc

Printer-friendly Version

Interactive Discussion

ence of chains of *Fragillariopsis kerguelensis*, *Eucampia Antarctica*, and *Chaetoceros Hyalochaeta* diatoms which contribute strongly to the larger autotrophic size fractions at many stations (L. Armand, personal communication, 2014). The presence of lipid-rich zooplankton in the two largest size fractions is another probable cause of their low ^{13}C -POC values, but one that we are unable to explore further.

To translate our observed ^{13}C -POC variations (in the autotrophic size classes) to growth rates using the relationships described in the Methods (Sect. 2.5.1), we must make some assumption about the size and shapes of the phytoplankton in the different filter fractions. This choice is difficult in the absence of detailed observations, and we took a very simple approach of representing the phytoplankton as rectangular prisms with square cross-sections, with the dimensions given in Table 3 for the 1, 5, 20 and 50 μm filter fractions. For the two larger fractions, we assumed diatoms were predominantly present as chains (based on microscopy; L. Armand, personal communication, 2014), and that the surface for CO_2 exchange was accordingly reduced (the details accompany Table 3). These assumptions are of course tenuous because diatom chains vary in their morphology, and of course the relationship between S/V and uptake is itself a large assumption. Nevertheless, on this basis, we obtained growth rate variations for each of the autotrophic size fractions (Table 2) and total community growth rates (Fig. 5) for each station by summing results for the four smallest size fractions (1, 5, 20, 50 μm). Similar variations across the stations were obtained by limiting the sum to the 5, 20, and 50 μm fraction results (data not shown). The growth rates decreased with size across the size fractions (from the 1 to the 50 μm filter) by factors of 10 to 15, in excellent agreement with allometric relationships assembled for a much broader range of phytoplankton, although the high growth rates of 2 to 3 d^{-1} in the smallest fraction are greater than expected for polar waters (Chisholm, 1992; C3zar and Echevarr3a, 2005).

Our community (sum of fractions) model growth rates compare reasonably well with a limited set of incubation results, calculated by integrating results from different light

BGD

11, 13841–13903, 2014

Chemometric perspectives on plankton community responses to natural iron fertilization

T. W. Trull et al.

Title Page

Abstract

Introduction

Conclusions

References

Tables

Figures

◀

▶

◀

▶

Back

Close

Full Screen / Esc

Printer-friendly Version

Interactive Discussion



level deck onboard incubations (Cavagna et al., 2014) over the depth of the surface mixed layers as shown in Table 4 (Park et al., 2014b).

The overall dynamic range of the incubation and model growth rates was identical (0.18 d^{-1}). For the model this ranged from 0.08 d^{-1} at the coldest early-sampled low biomass station over the plateau (A3–1) to 0.27 d^{-1} at coastal station TEW-2. The incubations ranged from a low value of 0.065 d^{-1} at the HNLC reference station (A3–1 was not studied) to a high of 0.24 d^{-1} at the Group 5 Polar Front station F-L (coastal stations were not studied). Overall correlation between the 8 pairs of results from the same stations (though not sampled at identical times) was very poor ($r^2 < 0.1$) but this was driven by strong disagreement at the single Group 5 downstream Polar Front station where the incubations found their highest depth integrated growth rate (0.24 d^{-1} at F-L) but our ^{13}C -based estimates were much lower, and without this pair, the correlation was reasonably strong ($r^2 = 0.67$).

Given the importance of S/V variations to the growth rate estimates, variations between Groups with similar size distributions and phytoplankton flora (the Group 1, 2 recirculation and Group 3 plateau stations) are probably more reliably assessed than variations between Groups with more distinct flora (coastal Group 4 stations and downstream Polar Front Group 5 stations). The Group 2 recirculation time series showed quite constant and moderate growth rates ($0.17\text{--}0.19 \text{ d}^{-1}$). Interestingly, values during the earlier Group 1 initial survey were somewhat higher in this region ($0.19\text{--}0.21 \text{ d}^{-1}$), and reached 0.23 d^{-1} at the southern end of the north-south transect over the plateau (TNS 9, 10). Later sampled Group 3 plateau stations (A3–2, G1, E4W, E4W2) also had high model growth rates ($0.19\text{--}0.24 \text{ d}^{-1}$).

These growth rate variations are in broad agreement with the development of blooms in these regions – in that the lowest biomass accumulation over the study period occurred in the recirculation, with higher values over the plateau. In contrast, the model suggests that the highest growth rates occurred in Group 4 coastal waters, where biomass accumulation was only moderate, and found only moderate growth rates for the Group 5 Polar Front stations where a strong bloom was already underway at the

Chemometric perspectives on plankton community responses to natural iron fertilization

T. W. Trull et al.

Title Page

Abstract

Introduction

Conclusions

References

Tables

Figures

◀

▶

◀

▶

Back

Close

Full Screen / Esc

Printer-friendly Version

Interactive Discussion



time of sampling (Fig. 2). It is not currently possible to determine why this misfit occurred, and it is not really surprising given the simplicity of the model and the complexity of the ecosystem dynamics. The misfit provides a useful cautionary note that the apparent growth rate variations have no real quantitative validity; at best they provide indicative information on the relative intensities of CO₂ assimilation across the Groups.

3.4 ¹⁵N variations

Similarly to the carbon isotopes, we discuss the ¹⁵N-PN variations relative to co-located ¹⁵N-NO₃ values ($^{15}\text{N-PN}_{\text{rs}} = ^{15}\text{N-PN} - ^{15}\text{N-NO}_3$), for the reasons outlined in the Methods (Sect. 2.5.2). As shown in Fig. 4, almost all the phytoplankton dominated size fractions (5–20, 20–50, 50–210 μm) had ¹⁵N-PN_{rs} values that fall between the upper bound of production from nitrate ($^{15}\text{N-PN}_{\text{rs}} = -4$) and the lower bound of production from ammonium ($^{15}\text{N-PN}_{\text{rs}} = -8$). There was also a tendency across all Groups towards lower ¹⁵N-PN_{rs} in the smaller phytoplankton fractions; consistent with greater use of ammonium by smaller phytoplankton (Armstrong, 1999; Karsh et al., 2003). The largest zoo-plankton containing size fractions (210–300, 300–1000 μm) had higher ¹⁵N-PN_{rs} values, which presumably result from the relatively large (~3‰) trophic enrichment that occurs in many marine organisms (Michener and Schell, 1994; Wada and Hattori, 1978). While these general variations with size held for all Groups, there were significant differences. In particular, the Group 3 plateau stations had the lowest ¹⁵N-PN_{rs} values for the larger autotrophic size classes (20–50 and 50–210 μm).

Using the end-member mixing model (Methods Sect. 2.5.2), we obtained the estimated community *f* ratios as shown in Fig. 5. The Group 3 plateau stations tended to have somewhat higher values (~0.7 vs. ~0.6) than the Group 5 downstream Polar Front bloom stations (TEW-7, TEW-8, and F-S); although this was not true for the highest biomass station (F-L). As with the growth rates, the Group 1 recirculation stations sampled early on the TNS transit were somewhat surprising in having relatively high values, though these were not observed on the later TEW transit or during the

Chemometric perspectives on plankton community responses to natural iron fertilization

T. W. Trull et al.

Title Page

Abstract

Introduction

Conclusions

References

Tables

Figures

◀

▶

◀

▶

Back

Close

Full Screen / Esc

Printer-friendly Version

Interactive Discussion



Chemometric perspectives on plankton community responses to natural iron fertilization

T. W. Trull et al.

[Title Page](#)[Abstract](#)[Introduction](#)[Conclusions](#)[References](#)[Tables](#)[Figures](#)[⏪](#)[⏩](#)[◀](#)[▶](#)[Back](#)[Close](#)[Full Screen / Esc](#)[Printer-friendly Version](#)[Interactive Discussion](#)

Group 2 time series. Finally, the coastal stations had high *apparent f* ratios, including values that exceed 1 (pointing to limitations of the model). Importantly, these high values are driven by the relatively low $^{15}\text{N-NO}_3$ values in these coastal waters, rather than by higher ^{15}N contents in their PON. The low $^{15}\text{N-NO}_3$ values are a surprise given the relatively low nitrate concentrations in these coastal waters (Fig. 6), suggesting other processes are at work. Our observations are insufficient to explain this. One possibility is delivery of low ^{15}N nitrate from sedimentary nitrification, but this still leaves open the question of why recently formed PN does not track the overall nitrate pool isotopic composition. Reliance on the *f* ratios from these coastal stations is thus not advisable. In contrast, comparison of our offshore *f* ratios to incubation results (Fig. 5; Cavagna et al., 2014) shows similar values and excellent correlation ($r^2 = 0.90$; provided the very low incubation based *f* ratio at the HNLC station R2 is discounted).

3.5 Nutrient depletion estimates

Surface water nutrient concentrations provide an initial perspective on the efficiency of the biological pump. Overall, the surface nitrate concentrations indicate lower values north than south of the Polar Front, but of course this may reflect longer term, larger region, controls on nitrate. Determination of the role of local recent biological activity in nitrate depletion requires a much closer examination. Figure 6 shows high spatial resolution maps of nitrate, temperature, and salinity obtained with the sensors operated continuously underway. Waters upstream from the plateau and south of the Polar Front were cold and saline with high nitrate concentrations, with these parameters reaching their highest values over the central plateau early in the voyage (near the Group 3 KEOPS bloom reference station A3–1), with temperature less than 2°C , salinity greater than 33.9, and nitrate above $30\ \mu\text{M}$. At the other extreme, Group 4 coastal waters had the lowest surface nitrates (below $10\ \mu\text{M}$), in association with very fresh (salinity < 33.6) and relatively warm ($> 3.5^\circ\text{C}$) waters. The Group 5 waters downstream in the bloom that formed north of the Polar Front well to the east (near $74\text{--}75^\circ\text{E}$ and the Group 5 stations TEW-7, -8, F-L and F-S), also had relatively low surface nitrates

(15–20 μM) and low salinities (33.7–33.8), and were quite warm ($> 4^\circ\text{C}$). In comparison, the Group 2 recirculation feature had intermediate nitrate concentrations between the plateau, coastal, and downstream Polar Front plume conditions.

These conditions evolved over the course of the study, with decreases in surface nitrate values being particularly strong (reaching 6–8 μM from winter conditions; Table 4) in regions of rapid biomass accumulation over the central plateau (especially along the plateau edge to the north of the A3 station) and in the bloom north of the Polar Front (near stations TEW-8, F-L, F-S). Low nitrate concentrations were also found in association with relatively low salinities to the southeast of the recirculation region, where the ship transited without station sampling. This appears to represent southward supply of waters from north of the Polar Front in association with its meandering (as also suggested by the satellite chlorophyll image sequences (Fig. 2 and animation in the Supplementary Materials, and by water parcel trajectories estimated from drifters and satellite altimetry; d'Ovidio et al., 2014). This process also appears to have driven warming and freshening in the recirculation over time. Thus nitrate budgets require partitioning of temporal changes driven by both hydrology and biology.

To separate local biological nitrate depletion from hydrological controls, we examined nitrate depletions in surface waters relative to estimates of initial winter nitrate concentrations for each station, as estimated from CTD profiles. We considered integrations to two different depths: (a) the frequently used choice (e.g. Arrigo et al., 1999; Sweeney et al., 2000) of the depth of the remnant winter water temperature minimum (T_{\min} -depth), and (b) shallower depths based on a threshold increase in salinity of 0.05 ($S_{\text{threshold}}$ -depth). This second choice was motivated by the presence of significant salinity gradients above the T_{\min} -depth (examples are shown in Fig. 7), particularly in waters near and north of the Polar Front, suggesting either that the most recent winter mixing was not as deep as previous years, or that horizontal mixing had brought fresher waters over the top of the T_{\min} , and thus in either case that nitrate depletion between the T_{\min} -depth and $S_{\text{threshold}}$ -depth was not attributable to recent consumption. Note that each of these nitrate depletion metrics reflects the sum of export since strati-

BGD

11, 13841–13903, 2014

Chemometric perspectives on plankton community responses to natural iron fertilization

T. W. Trull et al.

Title Page

Abstract

Introduction

Conclusions

References

Tables

Figures

◀

▶

◀

▶

Back

Close

Full Screen / Esc

Printer-friendly Version

Interactive Discussion

fication and the current standing stock, which may make a contribution to future export (at some unknown discounted rate owing to heterotrophic loss).

The two nitrate depletion metrics give differing views of the contributions to export from the different community Groups (as summarized in Fig. 8). Estimates based on the T_{\min} approach were much higher than those from the $S_{\text{threshold}}$ approach, because the T_{\min} -depth and was generally deeper and had higher nitrate than the $S_{\text{threshold}}$ -depth (Table 2). The T_{\min} approach also yielded more widely varying results within a Group, and suggested that the greatest depletion occurred for the downstream plume of Kerguelen island coastal waters that formed the bloom to the north of the Polar Front. In contrast, the $S_{\text{threshold}}$ approach identified the highest seasonal nitrate depletion as occurring over the central plateau, with somewhat lower values in the recirculation feature, followed by the Polar Frontal bloom and the reference station. These methodological differences were even larger for the silicic acid depletions (Fig. 8). This analysis underlines the importance of appropriate winter nitrate (and silicic acid) surface nitrate concentration estimates to the assignment of export magnitudes. We believe the $S_{\text{threshold}}$ approach is the most appropriate given the observed salinity stratification, especially for the relatively weak (deep, winter) thermal stratification observed in the Group 5 stations near the Polar Front. (Note that we could not estimate export for the Group 4 Kerguelen Island coastal stations because neither the T_{\min} nor the $S_{\text{threshold}}$ approaches were compatible with their shallow water columns). Both the T_{\min} and $S_{\text{threshold}}$ based nitrate depletions are relatively small as percentages of the initial upper water column inventories (2–18%; Table 4). This reflects the early seasonal sampling, as well as a significant extent of recycling via nitrification (Dehairs et al., 2014; Lasbleiz et al., 2014). Fractional depletions of silicate were higher (3–53%; data but not values shown in Table 4), consistent with the results of the autumn KEOPS expedition which revealed low nitrate removal but near complete Si depletion (Mosseri et al., 2008).

Our preferred $S_{\text{threshold}}$ nitrate depletion estimate can be further refined by removal of the standing stock of other nitrogen forms produced by the ecosystem (ammonium, urea, dissolved organic nitrogen, particulate nitrogen) to give a better estimate of N

BGD

11, 13841–13903, 2014

Chemometric perspectives on plankton community responses to natural iron fertilization

T. W. Trull et al.

Title Page

Abstract

Introduction

Conclusions

References

Tables

Figures

◀

▶

◀

▶

Back

Close

Full Screen / Esc

Printer-friendly Version

Interactive Discussion



proportion of the assimilated nitrogen is still present as standing stock (Fig. 8 bottom panel), and thirdly, there is some suggestion that more nitrogen than silicon is retained as standing stock (as a portion of depletion; compare the Fig. 8 middle and bottom panels).

4 Discussion

Our overall interest is to understand community responses to iron fertilisation, with a particular focus on ecosystem control of nutrient depletion and carbon export. We expect this response to vary as a function of iron inputs, but also possibly with time since fertilisation and its persistence (as a result of cascading trophic effects), and time of year (as a result of strong seasonality of the physical and biological background). Specific probable seasonal modulators of the response to iron include insolation, stratification, and the abundance of organisms with life cycles that resonate at the seasonal scale, e.g. larger zooplankton. In the following sections, we summarize the structure and function variations, relate them to temporal settings (as developed in the Methods section), and compare them to our estimates of nitrate (and silicic acid) depletion from surface waters as a proxy for carbon export.

4.1 Overview of community structure and function variations

Our size-fractionated chemometric parameters for microbial ecosystem structure and function identified significant differences among the various environments sampled by the KEOPS2 program. The upstream HNLC reference station (R2) displayed low phytoplankton abundance, relatively high BSi/POC ratios, slow growth rates (as indicated by strong discrimination against ^{13}C uptake), and ^{15}N -PN values suggesting that growth was predominantly on nitrate (although this result must be viewed with caution since it differs from the low f ratio obtained by incubation (Cavagna et al., 2014). These characteristics are consistent with its selection as a HNLC reference, but the total integrated

Chemometric perspectives on plankton community responses to natural iron fertilization

T. W. Trull et al.

Title Page

Abstract

Introduction

Conclusions

References

Tables

Figures

◀

▶

◀

▶

Back

Close

Full Screen / Esc

Printer-friendly Version

Interactive Discussion



biomass was higher than the lowest values seen in Southern Ocean HNLC waters and mesopelagic Ba levels indicated POC remineralization, possibly indicating a low-level early production event (Lasbleiz et al., 2014; Jacquet et al., 2014) as a result of a small degree of Fe fertilisation, possibly from particulate Fe inputs from the nearby Leclaire Rise (van der Merwe et al., 2014).

The moderate iron fertilisation of the recirculation feature downstream from the plateau (stations in Groups 1 and 2) increased growth rates by ~ 0.02 to 0.04 d^{-1} (Fig. 5) and biomass ~ 2 -fold (increasing from $\sim 50\%$ to 4-fold over time; Fig. 3), particularly in the larger phytoplankton size fractions (20–50 and 50–210 μm). There was no systematic change in BSi/POC ratios, with some stations showing lower values consistent with relief of iron limitation, but others showing higher values. Whether this resulted primarily from changes in species or the presence of empty frustules is unclear, although the analysis of depletions and standing stocks suggests loss of empty frustules (as did earlier work during KEOPS; Mosseri et al., 2008). This may reflect varying levels of low production coupled closely to export, as well as the possibility that production was in part limited by variations in mixed layer depth (Lasbleiz et al., 2014). The ^{15}N -PN observations indicated growth primarily on nitrate (as at the HNLC reference station).

Both of the more strongly iron fertilised offshore regions (the Group 3 central plateau and the Group 5 Polar Front bloom, Table 1.) exhibited increased growth rates in comparison to HNLC waters (elevated by $\sim 0.05 \text{ d}^{-1}$), but their community structures were quite different. The plateau stations exhibited most of their enhanced biomass in the largest phytoplankton size fraction (50–210 μm); whereas Polar Frontal biomass increases were dominated by the next smaller size (20–50 μm). This was also true for the very strongly Fe fertilised Group 4 coastal stations where growth rates were even more elevated (by 0.1 – 0.19 d^{-1} above the HNLC reference). Use of ammonium vs. nitrate was also different between the plateau and downstream Polar Frontal blooms, with the plateau stations using a greater proportion of nitrate.

Chemometric perspectives on plankton community responses to natural iron fertilization

T. W. Trull et al.

Title Page

Abstract

Introduction

Conclusions

References

Tables

Figures

◀

▶

◀

▶

Back

Close

Full Screen / Esc

Printer-friendly Version

Interactive Discussion



4.2 Links between community structure and export

Overall, one of the most important outcomes of our results regarding export (presented in Sect. 3.5 and Fig. 8) is that surface biomass is not a good guide to the history of export, i.e. the low biomass recirculation feature exhibited as much export as from the higher biomass Polar Front or Plateau blooms. This same conclusion was reached on the basis of sparse sediment trap deployments at 200 m depth (Laurenceau et al., 2014) and ^{234}Th depletions in surface waters, which identified the recirculation feature as having the highest C exports of all regions (Planchon et al., 2014).

The cause of the low export, at 200 m depth, from the Polar Front bloom (Group 5 downstream stations) may in part be the shallowness of its high biomass surface layer (only \sim half that of the recirculation feature and plateau; Lasbleiz et al., 2014; Laurenceau et al., 2014), allowing for more remineralisation before export through the 200 m depth horizon.

The cause of the high export from the low biomass recirculation feature is less easy to understand – it suggests that production (also found to be moderately high in these waters compared to the other regions; Cavagna et al., 2014) and export have been in close balance in these waters. This is a phenomenon often found in association with small phytoplankton dominated communities, and attributed to tight coupling with small grazers (Boyd and Newton, 1999; Cullen, 1995). Our observations show that this tight coupling also persisted as very large, moderately to heavily silicified diatoms (Fig. 3) became dominant. This suggests that tight coupling may have also been achieved for the larger phytoplankton. Notably there were abundant larger herbivorous zooplankton in the recirculation region (Carlotti et al., 2014), and large fecal pellets as well as diatom aggregates were important contributors to export, based on observations in polyacrylamide gel filled sediment traps (Laurenceau et al., 2014).

BGD

11, 13841–13903, 2014

Chemometric perspectives on plankton community responses to natural iron fertilization

T. W. Trull et al.

[Title Page](#)

[Abstract](#)

[Introduction](#)

[Conclusions](#)

[References](#)

[Tables](#)

[Figures](#)

[◀](#)

[▶](#)

[◀](#)

[▶](#)

[Back](#)

[Close](#)

[Full Screen / Esc](#)

[Printer-friendly Version](#)

[Interactive Discussion](#)



4.3 Influence of fertilisation time and persistence on ecosystem responses

As developed in the Methods section, we consider four possible relative indices for the nature of the Fe fertilization and the overall ecosystem responses:

i. Intensity of Fe fertilisation (lowest to highest):

recirculation feature < plateau <≈ Polar Front plume ≪ coastal stations

ii. Elapsed time since Fe fertilisation and its persistence (most recent to oldest):

Polar Front plume < recirculation feature <≈ plateau < coastal stations

iii. Magnitude of biomass accumulation (lowest to highest, at end of voyage):

recirculation feature < coastal stations < plateau <≈ Polar Front plume

iv. Elapsed time since initiation of biomass accumulation (most recent to oldest):

recirculation feature < Polar Front plume <≈ plateau ≪ coastal stations

If we put aside the coastal stations, where depletion and export could not be estimated, we can ask which of these might explain why the recirculation feature achieved high export in comparison to its low to moderate biomass and low to moderate intensity of iron fertilisation. Index (ii) emerges as the most likely candidate – the recirculation feature receives low intensity ongoing iron fertilisation as a result of the recirculation of waters along the Polar Front and into it from the northeast (D'Ovidio et al., 2014), with possible augmentations from shallow Ekman transport from the nearby Kerguelen shelf (D'Ovidio et al., 2014; Sanial et al., 2014). This is a fascinating possibility, because it suggests ecosystems are modulated differently by persistent as opposed to punctual inputs of Fe.

Index (iv) also lists the recirculation as an end-member, but it seems unlikely that lower biomass is of itself a driver of low export, given that many studies of export have found positive correlations with biomass, though with significant modulation by community structure, e.g. Boyd and Newton, 1995, 1999; Boyd and Trull, 2007; Buesseler, 1998; Buesseler et al., 2001, 2007.

Chemometric perspectives on plankton community responses to natural iron fertilization

T. W. Trull et al.

[Title Page](#)

[Abstract](#)

[Introduction](#)

[Conclusions](#)

[References](#)

[Tables](#)

[Figures](#)

[⏪](#)

[⏩](#)

[◀](#)

[▶](#)

[Back](#)

[Close](#)

[Full Screen / Esc](#)

[Printer-friendly Version](#)

[Interactive Discussion](#)

Do any of these indices also provide insight on why the community differs between the two strongly iron fertilised regions (the central plateau vs. the downstream Polar Front)? For size structure, none of the time perspectives (indices ii–iv) appears to help – the plateau and recirculation features with their dominance by very large diatoms (vs. the more balanced size structure of the coastal and downstream Polar Front bloom) do not fall appropriately along any of the time spectrums of these three “clocks”. To the extent that the intensity of iron fertilisation (index i) may have been higher in both coastal and Polar Front waters than over the plateau, despite similar current Fe levels (see the Methods section for discussion), this could provide an explanation, but it would imply that more Fe produces communities with smaller cells and thus be counter to the results of artificial iron experiments (Boyd et al., 1999, 2007). This leaves us with the strong possibility that the community structure differences between the plateau and Polar Front regions derive in part from other factors beyond levels, timing, or persistence of iron fertilisation.

5 Conclusions

A complex mosaic of phytoplankton blooms forms in response to natural iron fertilisation from the Kerguelen Plateau. Community structure variations in the downstream waters appear to have multiple influences, including the intensity and persistence of iron fertilisation, the progress of biomass accumulation, and possibly whether they were sourced from plateau vs. coastal waters. These differences developed even though phytoplankton growth rates appeared to increase more directly with the level of iron availability, pointing to additional influences from trophodynamics. These community effects strongly decoupled levels of surface biomass from levels of particle export to the ocean interior over the timescales of spring bloom development studied here.

Appendix A: Chemical and isotopic analyses

A1 Particle collection

The ship supply collected water from ~ 7 m depth via a 10 cm diameter plastic hose extended through a vertical stainless-steel stand-pipe protruding ~ 1 m below the ship's forward hull. A sealed rotary propeller pump drew the supply through a 1000 µm nylon cylindrical pre-filter and distributed it via a manifold at more than 50 L min⁻¹, with most water returned over the side. This pre-filter was cleaned before each sample, and then a manifold valve was opened to supply a smaller flow of 8–10 L min⁻¹ through our small volume bulk particle and large volume sequential filtration systems. The large volume size fractionation system passes the water through a 47 mm diameter 1000 µm screen (to remove any large particles that managed to pass through the pump pre-filter at higher flow rates), followed by 142 mm diameter Nitex nylon screens (300, 210, 50, 20, and 5 µm mesh sizes) and a final 142 mm diameter QMA quartz fibre filter (1 µm nominal pore size, Sartorius). The small volume bulk enclosed sample system rapidly fills a precisely known ~ 1 L volume and low pressure filters it through a QMA quartz filter (muffled and pre-loaded under clean conditions into in-line filter holders). Quartz filters were used in preference to glass to minimize ²³⁴Th backgrounds and to give better combustion characteristics during elemental and isotopic analysis. The flow path allowed a larger flow rate through the larger meshes (Table 2). The very minor amounts of material on the 1000 µm screen were not analysed. Particles on the other nylon screens were immediately resuspended (1 µm filtered seawater from the sampling location) and refiltered onto 25 mm diameter, 1.2 micron pore size silver membrane filters (Sterlitech) and, along with the QMA filter (Sartorius T293), were dried at 60 °C. Following drying, the particles were examined under stereo-microscopy onboard the ship at magnification up to 50x, and then analysed non-destructively onboard for ²³⁴Th activities (Planchon et al., 2014). All other analyses were carried out in the Hobart laboratories.

13874

BGD

11, 13841–13903, 2014

Chemometric perspectives on plankton community responses to natural iron fertilization

T. W. Trull et al.

Title Page

Abstract

Introduction

Conclusions

References

Tables

Figures

◀

▶

◀

▶

Back

Close

Full Screen / Esc

Printer-friendly Version

Interactive Discussion



A2 Particle analyses

Biogenic silica (BSi), Particulate organic carbon (POC), and particulate nitrogen (PN), $\delta^{13}\text{C}$ -POC, and $\delta^{15}\text{N}$ -PN analyses were carried out in Hobart. For BSi, a single 5 mm diameter punch of the silver filters was analysed using an approach similar to the methods of Paasche (1973) and Queguiner (2001). The biogenic silica was dissolved by adding 4 mL of 0.2 M NaOH and incubating at 95 °C for 90 min. Samples were then rapidly cooled to 4 °C and 1 mL of 1 M HCl was added. Thereafter samples were centrifuged at 1880 $\times g$ for 10 min and the supernatant was transferred to a new tube and diluted with artificial seawater (36 g L⁻¹ NaCl). Biogenic silica concentrations were determined by spectrophotometry using an Alpkem model 3590 segmented flow analyser and following USGS Method I-2700-85 with these modifications: ammonium molybdate solution contained 10 g L⁻¹ (NH₄)₆Mo₇O₂₄, 800 μL of 10 % sodium dodecyl sulphate detergent replaced Levor IV solution, acetone was omitted from the ascorbic acid solution, and artificial seawater was used as the carrier solution. Biogenic silica standard concentrations were 0 μM , 28 μM , 56 μM , 84 μM , 112 μM and 140 μM . Standard curves across all runs had an average slope of 48 438 \pm 454 (1 s.d. $n = 4$). The mean concentration of repeated check standards (140 μM) was 139.85 \pm 0.31 μM ($n = 68$). The average blank value was 0.009 \pm 0.006 $\mu\text{moles punch}^{-1}$ (1 s.d. $n = 5$), equating to 0.08 % of the mean of 50 μm fraction samples (highest concentrations) and 1.22 % of the mean of 300 μm fractions (lowest concentrations).

For the POC and PN analyses, 3 \times 5 mm punched sub-samples of the 25 mm diameter silver membrane filters were placed in acid-resistant silver capsules (Sercon SC0037), treated with two 10 μL aliquots of 2N HCl (and 2 \times 20 μL for the bulkier QMA filter sub-samples, 5 \times 5 mm punches) to remove carbonates (King et al., 1998), and dried at 60 °C. A first set of sub-samples was analysed for POC and PN concentrations by combustion of the encapsulated samples in a Thermo-Finnigan Flash 1112 elemental analyser with reference to sulphanilamide standards in the Central Sciences Laboratory of the University of Tasmania. Precision of the analyses was \sim 1 %, but

the overall precision was limited to 5–10% by the sub-sampling of the filters that often had patchy or uneven coverage. Based on the POC and PN results, a third set of sub-samples was punched for isotopic analyses with the number of punches adjusted to ensure similar voltages within the dynamic range of the spectrometer.

$\delta^{13}\text{C}$ -POC and $\delta^{15}\text{N}$ -PN on the silver filters were analysed separately using a Fisons NA1500 Elemental Analyser coupled via a Con-flow IV interface to a Finnigan Delta V^{PLUS} isotope ratio mass spectrometer at CSIRO Marine and Atmospheric Research with separate oxidation and reduction columns installed. For the QMA filters, a Flash 2000 EA1112 HT ThermoScientific was fitted with a single combined oxidation/reduction column with dead spaces minimised for improved precision at < 20 μg N. During all ^{15}N analyses, CO_2 was removed using a sodium hydroxide scrubber (self-indicating Ascarite 2, Thomas Scientific) to avoid CO^+ interference at m/z 29 and 28 (Brooks et al., 2003). The $\delta^{15}\text{N}$ and $\delta^{13}\text{C}$ isotopic compositions are expressed in delta notation vs. atmospheric N_2 and the VPDB standard, respectively. Standardization was by reference to CO_2 and N_2 working gases injected before and after each sample, with normalization to solid reference materials inserted (along with blank cups) after each 6 samples. For $\delta^{13}\text{C}$, the solid standards were NBS-22 oil (RM8539, -29.73‰) and NBS-19 (limestone, RM8544, +1.95‰), and casein (Protein Standard OAS B2155 batch 114 859, Elemental Microanalysis, $\delta^{13}\text{C}$ +5.94 and $\delta^{15}\text{N}$ -26.98). For $\delta^{15}\text{N}$, the solid standards were IAEA-N1 (ammonium sulphate, RM8547, +0.43‰) and IAEA-N3 (potassium nitrate, RM8549, +4.72‰) and casein (as above). Based on replicate analyses of these standards the estimated precisions were typically 0.1‰ or 1 standard deviation for both $\delta^{13}\text{C}$ ($n = 15$) and $\delta^{15}\text{N}$ ($n = 20$).

Sample replicates generally had comparable precisions to the reference materials, but filters with patchy coverage had lower precision (0.3‰ in the worst cases, presumably reflecting isotopic heterogeneity within the size fractions). In addition, a small correction (< +0.4‰) was made to the QMA filter results after indirect measurement of the blank (Avak and Fry, 1999) $\delta^{13}\text{C} = -29.6$ at $\sim 10\%$ of the sample signal strength. Procedural blanks were measured by passing 1 L of seawater through the onboard

BGD

11, 13841–13903, 2014

Chemometric perspectives on plankton community responses to natural iron fertilization

T. W. Trull et al.

Title Page

Abstract

Introduction

Conclusions

References

Tables

Figures

◀

▶

◀

▶

Back

Close

Full Screen / Esc

Printer-friendly Version

Interactive Discussion



pumping system and subsequent processing in parallel to the samples, and yielded negligible amounts of POC and PN (< 1 % of typical samples), and with ratios close to those of the samples, and no correction was applied.

A3 Dissolved component analyses

Underway nitrate concentrations were mapped using an ultra-violet nitrate sensor (ISUS V3, Satlantic), calibrated 3 times during the voyage against sea water nitrate standards (~ 15, 20, 25, 30 μM), with additional comparisons to nitrate samples collected from the underway supply at every station sampled for particle analyses, yielding precision of ~ 1.5 μM . Nitrate concentrations for these samples and the CTD-Niskin bottles were measured onboard using a segmented flow spectrometric autoanalyser, with precision of ~ 0.1 μM . The N and O isotopic compositions of dissolved nitrate were measured via its bacterial conversion to nitrate to nitrous oxide followed by isotope ratio mass spectrometry at the Vrije Universiteit Bruxelles, with precision of approximately 0.2‰ for $^{15}\text{N-NO}_3$ and of 0.4‰ for $^{18}\text{O-NO}_3$ (further analytical details are provided in Dehaers et al., 2014).

Samples for measurement of the carbon isotopic composition of dissolved inorganic carbon were collected in 10 mL Exetainer vials, with airtight septa, by filling the tubes from QMA filtered (~ 0.8 μm) underway supply and preserving them by addition of 20 μL of saturated mercuric chloride. 1 mL aliquots were withdrawn and injected into acid washed, helium flushed Exetainer tubes. 100 μL of ortho-phosphoric acid (99 %, Fluka) was injected and the headspace equilibrated at 25 °C for 18 h (modification of Assayag et al., 2006). Solid NBS19 CaCO_3 (200 to 230 μg , $\delta^{13}\text{C} = +1.98$, $n = 10$ standard deviation 0.02), and bulk quality assurance sediment trap material (1200 μg , 12.9 % CaCO_3 , $\delta^{13}\text{C} = +2.9$), was weighed into smooth wall tin capsules (5 × 5.5 mm SC1190, Sercon) and lowered into the Exetainer tubes, purged, then 1 mL of DIC free sea water added before proceeding as for the samples. Blank, standard and sample headspaces (one standard after each 5 samples) were sampled using a Finnigan GasBench2 (Thermo-scientific) fitted with a 100 μL sample loop. The headspace gases from the Gas Bench

13877

BGD

11, 13841–13903, 2014

Chemometric perspectives on plankton community responses to natural iron fertilization

T. W. Trull et al.

Title Page

Abstract

Introduction

Conclusions

References

Tables

Figures

◀

▶

◀

▶

Back

Close

Full Screen / Esc

Printer-friendly Version

Interactive Discussion



were analysed (continuous flow) by the DeltaV^{Plus} isotope ratio mass spectrometer and Isodat 3 software at CSIRO Marine and Atmospheric Research.

**The Supplement related to this article is available online at
doi:10.5194/bgd-11-13841-2014-supplement.**

5 *Acknowledgements.* The Institute Polaire Paul-Emile Victor, the captain and crew of the *Marion Dufresne*, the Australian Commonwealth Cooperative Research Centre Program, and CSIRO Marine and Atmospheric Research (CMAR) provided logistic and financial support. Special thanks to Pierre Sangiardi (IPEV) for implementing the underway seawater supply for our high volume particle sampling and underway sensor mapping; Louise Oriole (Laboratoire
10 d'Océanographie Microbienne, Banyuls sur mer, France) for shipboard nutrient analyses; Abraham Passmore (ACE CRC) for BSi analyses; Peter Jansen (IMOS) for the logging system for the underway ISUS ultra-violet nitrate sensor; Ben Weeding (IMOS) for advancing ISUS calibration; Thomas Rodemann for CHN analyses in the University of Tasmania Central Sciences Laboratory; VUB for nitrate isotope analyses, Clair Lo Monaco and Nicolas Metzl (LO-
15 CEAN, UPMC-CNRS) for access to $p\text{CO}_2$ results; and Andy Bowie (ACE CRC/UTAS), Pier van der Merwe (ACE CRC), and Fabien Queroue (UTAS/UBO) for access to iron results. This work was supported by the French Research program of INSU-CNRS LEFE-CYBER (Les enveloppes fluides et l'environnement – Cycles biogéochimiques, environnement et ressources), the French ANR (Agence Nationale de la Recherche, SIMI-6 program, ANR-10-BLAN-0614),
20 and the French CNES (Centre National d'Etudes Spatiales).

References

- Anderson, L. and Sarmiento, J.: Redfield ratios of remineralization determined by nutrient data analysis, *Global Biogeochem. Cy.*, 8, 65–80, 1994.
- 25 Armstrong, R. A.: An optimization-based model of iron-light-ammonium colimitation of nitrate uptake and phytoplankton growth, *Limnol. Oceanogr.*, 44, 1436–1446, 1999.

Chemometric perspectives on plankton community responses to natural iron fertilization

T. W. Trull et al.

Title Page

Abstract

Introduction

Conclusions

References

Tables

Figures

◀

▶

◀

▶

Back

Close

Full Screen / Esc

Printer-friendly Version

Interactive Discussion



Chemometric perspectives on plankton community responses to natural iron fertilization

T. W. Trull et al.

[Title Page](#)

[Abstract](#)

[Introduction](#)

[Conclusions](#)

[References](#)

[Tables](#)

[Figures](#)

[◀](#)

[▶](#)

[◀](#)

[▶](#)

[Back](#)

[Close](#)

[Full Screen / Esc](#)

[Printer-friendly Version](#)

[Interactive Discussion](#)

Arrigo, K. R., Robinson, D. H., Worthen, D. L., Dunbar, R. B., DiTullio, G. R., vanWoert, M., and Lizotte, M. P.: Phytoplankton community structure and the drawdown of nutrients and CO₂ in the Southern Ocean, *Science*, 283, 365–367, 1999.

Assmy, P., Smetacek, V., Montresor, M., Klaas, C., Henjes, J., Strass, V. H., Arrieta, J. M., Bathmann, U., Berg, G. M., and Breitbarth, E.: Thick-shelled, grazer-protected diatoms decouple ocean carbon and silicon cycles in the iron-limited Antarctic Circumpolar Current, *P. Natl. Acad. Sci. USA*, 110, 20633–20638, 2013.

Blain, S., Queguiner, B., and Trull, T.: The natural iron fertilization experiment KEOPS (Kerguelen Ocean and Plateau compared Study): an overview, *Deep-Sea Res. Pt. II*, 55, 559–565, 2008.

Blain, S., Capparos, J., Guéneuguès, A., Obernosterer, I., and Oriol, L.: Distributions and stoichiometry of dissolved nitrogen and phosphorus in the iron fertilized region near Kerguelen (Southern Ocean), *Biogeosciences Discuss.*, 11, 9949–9977, doi:10.5194/bgd-11-9949-2014, 2014.

Bowie, A., van der Merwe, P., Trull, T., Queroue, F., Fourquez, M., Planchon, F., Sarthou, G., and Blain, S.: Iron budgets for three distinct biogeochemical sites around the Kerguelen Plateau (Southern Ocean) during the natural fertilization experiment KEOPS-2, *Biogeosciences Discuss.*, in preparation, 2014.

Boyd, P. W. and Newton, P.: Evidence of the potential influence of planktonic community structure on the interannual variability of particulate carbon flux, *Deep-Sea Res. Pt. I*, 42, 619–639, 1995.

Boyd, P. W. and Newton, P.: Does planktonic community structure determine downward particulate organic carbon flux in different oceanic provinces?, *Deep-Sea Res. Pt. I*, 46, 63–91, 1999.

Boyd, P. W. and Trull, T. W.: Understanding the export of marine biogenic particles: is there consensus?, *Prog. Oceanogr.*, 4, 276–312, doi:10.1016/j.pocean.2006.10.007, 2007.

Boyd, P., Watson, A., Law, C. S., Abraham, E., Trull, T., and Murdoch, R.: SOIREE – a Southern Ocean iron release experiment elevates phytoplankton stocks in Polar waters, *EOS T. Am. Geophys. Un. Ocean Sci. Meet. Suppl.* 80, OS30, 1999.

Boyd, P. W., Jickells, T., Law, C. S., Blain, S., Boyle, E. A., Buesseler, K. O., Coale, K. H., Cullen, J. J., Baar, H. J. W.d., Follows, M., Harvey, M., Lancelot, C., Levasseur, M., Owens, N. P. J., Pollard, R., Rivkin, R. B., Sarmiento, J., Schoemann, V., Smetacek, V., Takeda, S., Tsuda, A., Turner, S., and Watson, A. J.: Mesoscale iron en-

Chemometric perspectives on plankton community responses to natural iron fertilization

T. W. Trull et al.

[Title Page](#)

[Abstract](#)

[Introduction](#)

[Conclusions](#)

[References](#)

[Tables](#)

[Figures](#)

[◀](#)

[▶](#)

[◀](#)

[▶](#)

[Back](#)

[Close](#)

[Full Screen / Esc](#)

[Printer-friendly Version](#)

[Interactive Discussion](#)



- Cózar, A. and Echevarría, F.: Size structure of the planktonic community in microcosms with different levels of turbulence, *Sci. Mar.*, 69, 187–197, 2005.
- Cullen, J. J.: Status of the iron hypothesis after the Open-Ocean Enrichment Experiment, *Limnol. Oceanogr.*, 40, 1336–1343, 1995.
- 5 de Baar, H. J. W., de Jong, J. T. M., Bakker, D. C. E., Loscher, B. M., Veth, C., Bathmann, U., and Smetacek, V.: Importance of iron for phytoplankton blooms and carbon dioxide drawdown in the Southern Ocean, *Nature*, 373, 412–415, 1995.
- Dehairs, F., Trull, T., Fernandez, C., Davies, D., Cavagna, A.-J., Planchon, F., Elskens, M., Roukaerts, A., Fonseca Batista, D., and Fripiat, F.: Nitrogen cycling in the Southern Ocean Kerguelen Plateau area: evidence for significant surface nitrification based on nitrate isotopic compositions, *Biogeosciences Discuss.*, in preparation, 2014.
- 10 D'Ovidio, F., et al.: Pathways of iron dispersion off the Kerguelen Plateau: the role of horizontal stirring, *Biogeosciences Discuss.*, in preparation, 2014.
- Georges, C., Monchy, S., Genitsaris, S., and Christaki, U.: Protist community composition during early phytoplankton blooms in the naturally iron-fertilized Kerguelen area (Southern Ocean), *Biogeosciences Discuss.*, 11, 11179–11215, doi:10.5194/bgd-11-11179-2014, 2014.
- 15 Goericke, R., Montoya, J. P., and Fry, B.: Physiology of isotopic fractionation in algae and cyanobacteria, in: *Stable Isotopes in Ecology and Environmental Science*, edited by: La jtha, K. and Michener, R. H., Blackwell Scientific Publications, Oxford, 1870–1221, 1994.
- Hoffmann, L. J., Peeken, I., and Lochte, K.: Effects of iron on the elemental stoichiometry during EIFEX and in the diatoms *Fragilariopsis kerguelensis* and *Chaetoceros dichaeta*, *Biogeosciences*, 4, 569–579, doi:10.5194/bg-4-569-2007, 2007.
- Hutchins, D. A. and Bruland, K. W.: Iron limited diatom growth and Si:N uptake ratios in a coastal upwelling regime, *Nature*, 393, 561–564, 1998.
- 25 Karsh, K. L., Trull, T. W., Lourey, A. J., and Sigman, D. M.: Relationship of nitrogen isotope fractionation to phytoplankton size and iron availability during the Southern Ocean Iron RElease Experiment (SOIREE), *Limnol. Oceanogr.*, 48, 1058–1068, 2003.
- Karsh, K. L., Trull, T. W., Sigman, D. M., Thompson, P. A., and Granger, J.: The contributions of nitrate uptake and efflux to isotope fractionation during algal nitrate assimilation, *Geochim. Cosmochim. Ac.*, 132, 391–412, 2014.
- 30 King, P., Kennedy, H., Newton, P., Jickells, T., Brand, T., Calvert, S., Cauwet, G., Etcheber, H., Head, B., Khripounoff, A., Manighetti, B., and Miquel, J. C.: Analysis of total and organic car-

Chemometric perspectives on plankton community responses to natural iron fertilization

T. W. Trull et al.

[Title Page](#)

[Abstract](#)

[Introduction](#)

[Conclusions](#)

[References](#)

[Tables](#)

[Figures](#)

[⏪](#)

[⏩](#)

[◀](#)

[▶](#)

[Back](#)

[Close](#)

[Full Screen / Esc](#)

[Printer-friendly Version](#)

[Interactive Discussion](#)

- Park, Y.-H., Roquet, F., Fuda, J.-L., and Durand, I.: Large scale circulation over and around the Kerguelen Plateau, *Deep-Sea Res. Pt. II*, 55, 566–581, 2008.
- Park, Y.-H., Lee, J.-H., Durand, I., and Hong, C.-S.: Validation of the Thorpe scale-derived vertical diffusivities against microstructure measurements in the Kerguelen region, *Biogeosciences Discuss.*, 11, 12137–12157, doi:10.5194/bgd-11-12137-2014, 2014a.
- Park, Y.-H., Durand, I., Kestenare, E., Rougier, G., Zhou, M., d'Ovidio, F., Cotte, C., and Lee, J.-H.: Polar front around the Kerguelen Islands: an up-to-date determination and associated circulation of surface/subsurface waters, *J. Geophys. Res.*, submitted, 2014b.
- Planchon, F., Ballas, D., Cavagna, A.-J., Bowie, A., Davies, D., Trull, T., Laurenceau, E., van der Merwe, P., and Dehairs, F.: Carbon export in the naturally iron-fertilized Kerguelen area of the Southern Ocean based on the ^{234}Th approach, *Biogeosciences Discuss.*, in preparation, 2014.
- Pollard, R., Sanders, R., Lucas, M., and Statham, P.: The Crozet Natural Iron Bloom and Export Experiment (CROZEX), *Deep-Sea Res. Pt. II*, 54, 1905–1914, doi:10.1016/j.dsr2.2007.07.023, 2007.
- Popp, B. N., Laws, E. A., Bidigare, R. R., Dore, J. E., Hanson, K. L., and Wakeham, S. G.: Effect of phytoplankton cell geometry on carbon isotopic fractionation, *Geochim. Cosmochim. Ac.*; 62, 69–77, 1998.
- Popp, B. N., Trull, T., Kenig, F., Wakeham, S. G., Rust, T. M., Tilbrook, B., Griffiths, F. B., Wright, S. W., Marchant, H. J., Bidigare, R. R., and Laws, E. A.: Controls on the carbon isotopic composition of Southern Ocean phytoplankton, *Global Biogeochem. Cy.*, 13, 827–843, 1999.
- Queguiner, B.: Biogenic silica production in the Australian sector of the Subantarctic Zone of the Southern Ocean in late summer 1998, *J. Geophys. Res.*, 106, 31627–31636, 2001.
- Queguiner, B.: Iron fertilization and the structure of planktonic communities in high nutrient regions of the Southern Ocean, *Deep-Sea Res. Pt. II*, 90, 43–54, 2013.
- Queroue, F., Sarthou, G., Chever, F., van der Merwe, P., Lannuzel, D., Townsend, A., Bucciarelli, E., Planquette, H., Cheize, M., Blain, D., d'Ovidio, F., and Bowie, A.: A new study of natural Fe fertilization processes in the vicinity of the Kerguelen Islands (KEOPS2 experiment), *Biogeosciences Discuss.*, in preparation, 2014.
- Ragueneau, O., Schultes, S., Bidle, K., Claquin, P., and Moriceau, B.: Si and C interactions in the world ocean: importance of ecological processes and implications for the role of diatoms

Chemometric perspectives on plankton community responses to natural iron fertilization

T. W. Trull et al.

[Title Page](#)[Abstract](#)[Introduction](#)[Conclusions](#)[References](#)[Tables](#)[Figures](#)[◀](#)[▶](#)[◀](#)[▶](#)[Back](#)[Close](#)[Full Screen / Esc](#)[Printer-friendly Version](#)[Interactive Discussion](#)

in the biological pump, *Global Biogeochem. Cy.*, 20, GB4S02, doi:10.1029/2006GB002688, 2006.

Rau, G. H., Riebesell, U., and Wolf-Gladrow, D.: CO_{2aq}-dependent photosynthetic ¹³C fractionation in the ocean: a model versus measurements, *Global Biogeochem. Cy.*, 11, 267–278, 1997.

Redfield, A. C., Ketchum, B. H., and Richards, F. H.: The influence of organisms on the composition of seawater, in: *The Sea*, edited by: Hill, M. N., Inter-Science, New York, 26–77, 1963.

Sanial, V., van Beek, P., Lansard, B., Souhout, M., and Kestenare, E.: Use of Ra isotopes to deduce rapid transfer of sediment derived inputs off the Kerguelen Plateau, *Biogeosciences Discuss.*, in preparation, 2014.

Savoie, N., Trull, T. W., Jacquet, S. H. M., Navez, J., and Dehairs, F.: Th-234-based export fluxes during a natural iron fertilization experiment in the Southern Ocean (KEOPS), *Deep-Sea Res. Pt. II*, 55, 841–855, 2008.

Smetacek, V.: Role of sinking in diatom life-history cycles: ecological, evolutionary and geological significance, *Mar. Biol.*, 84, 239–251, 1985.

Smetack, V.: Diatoms and the silicate factor, *Nature*, 391, 224–225, 1998.

Sokolov, S. and Rintoul, S. R.: Circumpolar structure and distribution of the Antarctic Circumpolar Current fronts: 1. Mean circumpolar paths, *J. Geophys. Res.*, 114, C11018, doi:10.1029/2008JC005108, 2009.

Sweeney, C., Hansell, D. A., Carlson, C. A., Codispoti, L. A., Gordon, L. I., Marra, J., Millero, F. J., Smith, W. O., and Takahashi, T.: Biogeochemical regimes, net community production and carbon export in the Ross Sea, Antarctica, *Deep-Sea Res. Pt. II*, 47, 3369–3394, 2000.

Syvaranta, J. and Rautio, M.: Zooplankton, lipids and stable isotopes: importance of seasonal, latitudinal, and taxonomic differences, *Can. J. Fish. Aquat. Sci.*, 67, 1721–1729, 2010.

Takeda, S.: Influence of iron availability on nutrient consumption ratio of diatoms in oceanic waters, *Nature*, 393, 774–777, 1998.

Trull, T. W. and Armand, L.: Insights into Southern Ocean carbon export from the delta C-13 of particles and dissolved inorganic carbon during the SOIREE iron release experiment, *Deep-Sea Res. Pt. II*, 48, 2655–2680, 2001.

Chemometric perspectives on plankton community responses to natural iron fertilization

T. W. Trull et al.

Title Page

Abstract

Introduction

Conclusions

References

Tables

Figures

◀

▶

◀

▶

Back

Close

Full Screen / Esc

Printer-friendly Version

Interactive Discussion



Trull, T. W., Davies, D., and Casciotti, K.: Insights into nutrient assimilation and export in naturally iron-fertilized waters of the Southern Ocean from nitrogen, carbon and oxygen isotopes, *Deep-Sea Res. Pt. II*, 55, 820–840, 2008.

5 van der Merwe, P., Bowie, A. R., Qu  rou  , F., Armand, L., Blain, S., Chever, F., Davies, D., Dehairs, F., Planchon, F., Sarthou, G., Townsend, A. T., and Trull, T.: Sourcing the iron in the naturally-fertilised bloom around the Kerguelen Plateau: particulate trace metal dynamics, *Biogeosciences Discuss.*, 11, 13389–13432, doi:10.5194/bgd-11-13389-2014, 2014.

Wada, E. and Hattori, A.: Nitrogen isotope effects in the assimilation of inorganic nitrogenous compounds by marine diatoms, *Geomicrobiol. J.*, 1, 85–101, 1978.

10 Weiss, R. F.: Carbon dioxide in water and seawater: the solubility of a non-ideal gas, *Mar. Chem.*, 2, 203–215, 1974.

BGD

11, 13841–13903, 2014

Chemometric perspectives on plankton community responses to natural iron fertilization

T. W. Trull et al.

Table 1. Station Groups.

Group	Map colour ¹	Group name	Timing in voyage	Biomass ²	Fe Supply ³
1	blue	recirculation survey and HNLC	early	low	low
2	green	recirculation time series	early through late	low	mod.
3	yellow	plateau	early + late	mod. to high	mod. to high
4	red	coastal	early	mod., stable	very high
5	purple	downstream Polar Front	middle + late	high	mod. to high

¹ Figure 1 shows a map of station locations.

² Figure 2 shows biomass distributions at the time of sampling and the animation (Supplement) shows seasonal timing of it's accumulation.

³ The timing of Fe supply is discussed in the text.

[Title Page](#)
[Abstract](#)
[Introduction](#)
[Conclusions](#)
[References](#)
[Tables](#)
[Figures](#)
[Back](#)
[Close](#)
[Full Screen / Esc](#)
[Printer-friendly Version](#)
[Interactive Discussion](#)


Table 2. Chemometric results for size-fractionated particles.

Station Date/location group	Volume L	fraction µm	POC µM	PN µM	PBSi µM	POC/ PN atom	PBSi/ POC atom	PBSi/ PN atom	$\delta^{13}\text{C}_{\text{POC}}$ ‰ _{v-PDB}	$\delta^{13}\text{C}_{\text{POC}}-\delta^{13}\text{C}_{\text{DIC}}$ ‰ _{v-PDB}	$\delta^{15}\text{N}_{\text{PN}}$ ‰ _{air}	$\delta^{15}\text{N}_{\text{PN}}-\delta^{15}\text{N}_{\text{NO}_3}$ ‰ _{air}	f ratio	growth rate d ⁻¹ [CO ₂] _{aq}
A3 1	1181	300	0.01	0.00	0.00	11.15	0.21	2.30	-25.01	-26.24	#N/A	#N/A		
20 Nov 2011	1181	210	0.02	0.00	0.00	6.46	0.17	1.13	-26.16	-27.39	3.97	-2.12		
50.6300° E	184	50	0.73	0.13	0.60	5.62	0.83	4.65	-23.09	-24.32	1.16	-4.93	0.77	0.07
72.0800° S	184	20	0.65	0.10	0.50	6.29	0.76	4.79	-22.09	-23.32	-0.28	-6.37	0.41	0.22
group3	184	5	0.14	0.02	0.08	7.91	0.58	4.57	-24.25	-25.49	0.37	-5.72	0.57	0.58
	184	1	1.74	0.33	0.53	5.29			-27.07	-28.31	2.39	-3.70	1.08	0.89
		total	3.29	0.58	1.19	5.63	0.77	4.65	-25.07		1.59		0.87	0.08
		bulk	3.55	0.64	5.52					1.23		6.09		24.23
TNS 10	1599	300	0.02	0.00	0.01	6.53	0.32	2.11	-24.35	-25.62	2.64	-3.59		
21 Oct 2011	1599	210	0.02	0.00	0.01	6.17	0.36	2.25	-25.30	-26.57	2.57	-3.66		
50.2142° E	271	50	0.77	0.14	0.62	5.70	0.80	4.56	-22.55	-23.81	0.60	-5.63	0.59	0.21
72.1320° S	271	20	0.42	0.07	0.33	5.93	0.78	4.63	-22.38	-23.65	-0.18	-6.41	0.40	0.56
group3	271	5	0.12	0.02	0.07	6.94	0.57	3.99	-24.02	-25.28	0.48	-5.75	0.56	1.04
	271	1	1.42	0.26	0.53	5.53			-26.61	-27.88	2.49	-3.74	1.07	2.27
		total	2.77	0.49	1.03	5.69	0.76	4.48	-24.70		1.51		0.82	0.23
		bulk	3.86	0.74	5.20					1.27		6.23		23.63
TNS 09	869	300	0.03	0.00	0.01	6.84	0.23	1.58	-24.63	-25.93	3.47	-2.86		
21 Oct 2011	869	210	0.09	0.02	0.03	5.40	0.30	1.60	-25.77	-27.07	3.11	-3.22		
49.7991° E	42	50	11.60	1.82	9.84	6.37	0.85	5.41	-22.57	-23.87	1.25	-5.08	0.73	0.21
72.2002° S	42	20	1.87	0.27	1.64	7.02	0.88	6.16	-22.32	-23.62	1.54	-4.79	0.80	0.56
group3	42	5	0.81	0.12	0.45	7.03	0.55	3.90	-23.15	-24.45	1.00	-5.33	0.67	1.11
	42	1	8.53	1.40	6.11	6.33	0.83	5.38	-26.52	-27.82	1.20	-5.13	0.72	2.29
		total	22.92	3.62	11.96	6.33	0.83	5.38	-24.06		1.26		0.73	0.23
		bulk	6.97	1.17	5.98					1.30		6.33		23.63
TNS 08	997	300	0.04	0.01	0.01	5.47	0.23	1.25	-24.13	-25.44	3.98	-2.44		
21 Oct 2011	997	210	0.12	0.02	0.02	5.03	0.15	0.73	-25.35	-26.66	3.45	-2.97		
49.4628° E	216	50	1.46	0.23	1.18	6.37	0.80	5.12	-23.81	-25.12	1.75	-4.67	0.83	0.19
72.2401° S	216	20	0.60	0.09	0.51	6.93	0.85	5.91	-22.27	-23.58	1.90	-4.52	0.87	0.56
group1	216	5	0.18	0.03	0.11	6.82	0.62	4.21	-23.59	-24.90	0.82	-5.60	0.60	1.07
	216	1	2.77	0.49	5.60	5.60			-26.00	-27.31	0.20	-6.22	0.44	2.42
		total	5.18	0.87	1.83	5.96	0.76	4.88	-24.83		0.92		0.60	0.21
		bulk	6.14	1.09	5.61					1.31		6.42		23.63
TNS 06	1025	300	0.03	0.00	0.00	6.26	0.06	0.40	-24.77	-26.09	3.77	-2.57		
22 Oct 2011	1025	210	0.05	0.01	0.01	5.02	0.18	0.89	-24.92	-26.25	3.75	-2.59		
48.7989° E	110	50	1.56	0.27	0.88	5.86	0.57	3.32	-23.14	-24.46	2.29	-4.05	0.99	0.19
72.3006° S	110	20	0.93	0.14	0.58	6.49	0.63	4.08	-22.63	-23.96	2.15	-4.19	0.95	0.54
group1	110	5	0.34	0.05	0.14	6.93	0.42	2.91	-24.25	-25.57	1.31	-5.03	0.74	0.99
	110	1	4.30	0.85	5.04	5.04			-26.31	-27.63	0.09	-6.25	0.44	2.28
		total	7.20	1.33	1.62	5.43	0.56	3.43	-25.04		0.84		0.62	0.21
		bulk	4.73	0.79	6.02					1.33		6.34		23.18
TNS 05	1081	300	0.03	0.01	0.01	5.67	0.20	1.11	-24.28	-25.55	4.06	-2.18		
22 Oct 2011	1081	210	0.07	0.02	0.01	4.80	0.08	0.39	-25.18	-26.45	4.06	-2.18		
48.4677° E	151	50	1.04	0.19	0.78	5.50	0.75	4.14	-24.73	-26.01	2.16	-4.08	0.98	0.17
72.2018° S	151	20	0.61	0.09	0.51	6.53	0.84	5.50	-22.95	-24.23	2.06	-4.18	0.95	0.52
group1	151	5	0.28	0.04	0.17	6.72	0.61	4.11	-23.81	-25.08	1.26	-4.98	0.76	1.03
	151	1	2.66	0.49	5.48	5.48			-26.64	-27.92	0.45	-5.79	0.55	2.20
		total	4.68	0.83	1.48	5.65	0.73	4.29	-25.54		1.15		0.71	0.19
		bulk	4.20	0.75	5.62					1.27		6.24		23.18

Chemometric perspectives on plankton community responses to natural iron fertilization

T. W. Trull et al.

Title Page

Abstract Introduction

Conclusions References

Tables Figures

◀ ▶

◀ ▶

Back Close

Full Screen / Esc

Printer-friendly Version

Interactive Discussion



Table 2. Continued.

Station Date/location group	Volume L	fraction µm	POC µM	PN µM	PBSi µM	POC/ PN atom	PBSi/ POC atom	PBSi/ PN atom	$\delta^{13}\text{CPOC}$ ‰ _{ov-PDB}	$\delta^{13}\text{CPOC}-\delta^{13}\text{CDIC}$ ‰ _{ov-PDB}	$\delta^{15}\text{NPN}$ ‰ _{air}	$\delta^{15}\text{NPN}-\delta^{15}\text{NO}_3$ ‰ _{air}	$\delta^{15}\text{NO}_3$ ‰ _{air}	f ratio	growth rate d ⁻¹ [CO ₂] _{aq}
TNS 03	975	300	0.03	0.01	0.01	6.14	0.31	1.88	-25.91	-27.16	3.33	-2.87			
23 Oct 2011	975	210	0.02	0.00	0.01	7.00	0.54	3.82	-25.41	-26.66	3.29	-2.91			
47.8336° E	165	50	0.91	0.16	0.66	5.82	0.73	4.25	-22.98	-24.23	1.74	-4.46	0.89	0.19	
71.9196° S	165	20	0.45	0.07	0.31	6.79	0.69	4.67	-22.98	-24.23	1.28	-4.92	0.77	0.51	
group1	165	5	0.17	0.02	0.06	8.09	0.38	3.07	-24.07	-25.32	0.75	-5.45	0.64	0.99	
	165	1	2.95	0.54		5.51			-26.96	-28.21	1.17	-5.03	0.74	2.07	
		total	4.54	0.79	1.06	5.76	0.67	4.20	-25.64		1.30		0.77	0.21	
		bulk	4.04	0.69		5.83				1.25		6.20		0.77	22.75
TNS 02	784	300	0.01	#N/A	0.00	#N/A	0.20	#N/A	-26.60	-27.93	#N/A	#N/A			
23 Oct 2011	784	210	0.01	0.00	0.00	10.77	0.20	2.19	-25.99	-27.32	#N/A	#N/A			
47.3318° E	170	50	0.17	0.02	0.07	8.20	0.43	3.57	-23.46	-24.79	2.57	-3.81	1.05	0.18	
71.7013° S	170	20	0.40	0.06	0.15	6.32	0.38	2.38	-21.95	-23.28	1.89	-4.49	0.88	0.55	
group5	170	5	0.12	0.02	0.04	6.98	0.32	2.27	-25.54	-26.87	1.93	-4.45	0.89	0.85	
	170	1	2.91	0.53		5.45			-26.09	-27.43	1.32	-5.06	0.73	2.27	
		total	3.62	0.64	0.27	5.69	0.38	2.61	-25.50		1.43		0.76	0.21	
		bulk	2.60	0.44		5.92				1.33		6.38		0.76	22.75
TNS 01	1279	300	0.03	0.01	0.00	5.53	0.03	0.18	-25.14	-25.93	3.32	-3.62			
23 Oct 2011	1279	210	0.02	0.00	0.00	7.21	0.11	0.81	-26.26	-27.05	1.53	-5.41			
46.8333° E	256	50	0.16	0.02	0.05	6.77	0.30	2.03	-25.66	-26.45	1.12	-5.82	0.54	0.16	
71.5011° S	256	20	0.19	0.03	0.07	6.83	0.39	2.68	-25.02	-25.81	1.71	-5.23	0.69	0.45	
group5	256	5	0.13	0.02	0.04	7.22	0.34	2.43	-24.86	-25.65	1.70	-5.24	0.69	0.96	
	256	1	2.88	0.52		5.52			-26.04	-26.83	-0.34	-7.28	0.18	2.42	
		total	3.40	0.60	0.17	5.69	0.32	2.19	-25.92		-0.09		0.23	0.18	
		bulk	3.70	0.59		6.32				0.79		6.94		0.23	23.05
R 2	2685	300	0.00	0.00	0.00	10.90	0.26	2.85	-25.76	-27.07	#N/A	#N/A			
26 Oct 2011	2685	210	0.01	0.00	0.00	9.92	0.37	3.70	-28.86	-30.18	1.56	-4.92			
50.3587° E	167	50	0.45	0.07	0.23	6.23	0.50	3.11	-25.66	-26.97	1.73	-4.75	0.81	0.15	
66.7168° S	167	20	0.31	0.04	0.18	6.94	0.58	4.06	-24.84	-26.16	2.28	-4.20	0.95	0.44	
group1	167	5	0.16	0.02	0.06	8.73	0.38	3.35	-25.64	-26.96	0.90	-5.58	0.60	0.85	
	167	1	2.89	0.51	#N/A	5.71			-28.14	-29.45	0.84	-5.64	0.59	1.80	
		total	3.82	0.64	0.47	5.94	0.51	3.46	-27.48		1.04		0.64	0.17	
		bulk	2.37	0.40		5.95				1.31		6.48		0.64	22.85
E 1 day	1209	300	0.02	0.00	0.00	7.07	0.20	1.43	-23.28	-24.65	3.04	-3.36			
29 Oct 2011	1209	210	0.07	0.01	0.03	5.51	0.40	2.18	-25.75	-27.12	2.42	-3.98			
48.4664° E	181	50	1.92	0.31	1.14	6.18	0.59	3.67	-23.52	-24.89	1.94	-4.46	0.88	0.17	
72.1993° S	181	20	0.57	0.09	0.36	6.64	0.63	4.20	-23.29	-24.66	2.03	-4.37	0.91	0.47	
group2	181	5	0.15	0.02	0.05	6.97	0.34	2.34	-24.73	-25.10	0.90	-5.50	0.62	0.88	
	181	1	3.64	0.62		5.87			-26.81	-28.18	-0.25	-6.65	0.34	2.00	
		total	6.36	1.05	1.58	6.05	0.58	3.65	-25.43		0.64		0.55	0.19	
		bulk	4.85	0.78		6.19				1.37		6.40		0.55	21.88
E 1 night	2449	300	0.48	0.11	0.03	4.45	0.06	0.28	-24.26	-25.48	3.24	-3.28			
29 Oct 2011	2449	210	0.33	0.06	0.12	5.26	0.37	1.94	-24.82	-26.03	2.48	-4.04			
48.4664° E	310	50	3.45	0.57	1.56	6.10	0.45	2.76	-23.88	-25.10	1.91	-4.61	0.85	0.17	
72.1993° S	310	20	0.40	0.06	0.18	6.64	0.44	2.95	-23.55	-24.76	1.96	-4.56	0.86	0.47	
group2	310	5	0.10	0.01	0.03	6.85	0.33	2.25	-24.62	-25.83	0.98	-5.54	0.62	0.90	
	310	1	3.45	0.58		5.90			-26.79	-28.00	-0.04	-6.56	0.36	2.04	
		total	8.21	1.40	1.92	5.88	0.40	2.37	-25.16		1.21		0.61	0.19	
		bulk	5.11	0.79		6.45				1.22		6.52		0.61	21.88

Chemometric perspectives on plankton community responses to natural iron fertilization

T. W. Trull et al.

Title Page

Abstract Introduction

Conclusions References

Tables Figures

⏪ ⏩

⏴ ⏵

Back Close

Full Screen / Esc

Printer-friendly Version

Interactive Discussion



Table 2. Continued.

Station Date/location group	Volume L	fraction µm	POC µM	PN µM	PBSi µM	POC/ PN atom	PBSi/ POC atom	PBSi/ PN atom	$\delta^{13}\text{CPOC}$ ‰ _{v-PDB}	$\delta^{13}\text{CPOC}-\delta^{13}\text{CDIC}$ ‰ _{v-PDB}	$\delta^{15}\text{NPN}$ ‰ _{air}	$\delta^{15}\text{NPN}-\delta^{15}\text{NO}_3$ ‰ _{air}	f ratio	growth rate d ⁻¹ [CO ₂] _{aq}
TEW 1	1516	300	0.03	0.01	0.00	5.06	0.08	0.39	-21.37	-22.85	5.05	-1.52		
31 Oct 2011	1516	210	0.03	0.01	0.01	4.88	0.19	0.91	-20.62	-22.10	3.78	-2.79		
49.1502° E	59	50	2.19	0.39	1.07	5.62	0.49	2.75	-19.66	-21.14	3.19	-3.38	1.15	0.23
69.8323° S	59	20	4.02	0.69	2.11	5.83	0.52	3.06	-19.36	-20.84	3.04	-3.53	1.12	0.64
group4	59	5	1.68	0.29	0.97	5.90	0.57	3.39	-20.44	-21.92	2.79	-3.78	1.05	1.25
	59	1	6.34	0.93		6.82			-22.88	-24.36	2.11	-4.46	0.89	2.96
		total	14.29	2.30	4.15	6.20	0.52	3.02	-21.10		2.66		1.02	0.26
		bulk	9.29	1.57		5.93				1.48		6.57		22.17
TEW 2	650	300	0.02	0.00	0.00	6.18	0.04	0.28	-23.47	-24.86	#N/A	#N/A		
31 Oct 2011	650	210	0.02	0.00	0.00	5.88	0.21	1.24	-23.34	-24.74	3.52	-2.89		
48.8994° E	161	50	0.88	0.14	0.33	6.21	0.37	2.31	-19.09	-20.48	2.37	-4.04	0.99	0.24
70.6663° S	161	20	2.16	0.36	0.63	6.09	0.29	1.77	-19.18	-20.57	2.20	-4.21	0.95	0.65
group4	161	5	0.13	0.02	0.09	7.25	0.64	4.67	-22.24	-23.63	2.41	-4.00	1.00	1.11
	161	1	3.33	0.50	#N/A	6.64			-24.10	-25.49	1.88	-4.53	0.87	2.68
		total	6.53	1.02	1.05	6.39	0.33	2.01	-21.76		2.07		0.92	0.27
		bulk	8.14	1.33		6.11				1.39		6.41		22.17
TEW 3	981	300	0.09	0.02	0.00	4.15	0.01	0.04	-23.87	-25.09	4.05	-1.90		
31 Oct 2011	981	210	0.01	0.00	0.00	5.58	0.17	0.97	-25.01	-26.23	#N/A	#N/A		
48.7991° E	93	50	0.11	0.02	0.06	5.82	0.52	3.05	-24.46	-25.67	#N/A	#N/A	#N/A	0.16
71.0176° S	93	20	0.74	0.12	0.32	6.23	0.43	2.69	-22.39	-23.61	1.99	-3.96	1.01	0.52
group4	93	5	0.14	0.02	0.05	7.86	0.35	2.76	-23.54	-24.75	1.93	-4.02	1.00	1.01
	93	1	8.01	1.27		6.30			-25.92	-27.13	1.19	-4.76	0.81	2.28
		total	9.10	1.45	0.43	6.28	0.40	2.41	-25.56		1.29		0.83	0.19
		bulk	6.26	0.89		7.04				1.21		5.95		22.17
TEW 4	1150	300	0.64	0.13	0.11	4.87	0.17	0.84	-24.66	-25.32	3.65	-2.84		
1 Nov 2011	1150	210	0.65	0.13	0.22	5.05	0.34	1.72	-24.36	-25.02	2.59	-3.90		
48.6331° E	88	50	5.10	0.84	2.28	6.11	0.45	2.72	-23.84	-24.50	2.02	-4.47	0.88	0.18
71.6170° S	88	20	1.27	0.21	0.57	6.18	0.45	2.77	-22.69	-23.35	1.76	-4.73	0.82	0.53
group1	88	5	0.26	0.04	0.10	5.93	0.39	2.31	-23.67	-24.33	1.07	-5.42	0.64	1.05
	88	1	7.95	1.45		5.48			-25.79	-26.45	0.37	-6.12	0.47	2.45
		total	15.89	2.80	3.28	5.68	0.41	2.44	-24.77		1.23		0.64	0.21
		bulk	9.41	1.73		5.43				0.66		6.49		22.17
E 2	1748	300	0.20	0.04	0.01	4.38	0.03	0.14	-21.25	-22.57	2.68	-3.94		
1 Nov 2011	1748	210	0.06	0.01	0.01	4.65	0.09	0.42	-24.76	-26.08	2.99	-3.63		
48.5234° E	123	50	1.44	0.25	0.63	5.71	0.44	2.52	-24.85	-26.17	1.62	-5.00	0.75	0.16
72.0771° S	123	20	1.26	0.20	0.50	6.22	0.40	2.49	-23.58	-24.90	1.64	-4.98	0.75	0.47
group2	123	5	0.30	0.05	0.10	6.38	0.33	2.10	-23.94	-25.26	1.02	-5.60	0.60	0.97
	123	1	5.60	1.01		5.55			-26.27	-27.59	-0.52	-7.14	0.22	2.17
		total	8.85	1.57	1.25	5.65	0.38	2.24	-25.46		0.27		0.39	0.18
		bulk	6.78	1.21		5.62				1.32		6.62		22.17
TEW 5	1748	300	0.26	0.06	0.00	4.39	0.01	0.02	-25.67	-27.05	4.18	-2.60		
1 Nov 2011	1748	210	0.05	0.01	0.00	4.57	0.06	0.28	-24.90	-26.27	3.33	-3.45		
48.4678° E	123	50	1.28	0.21	0.54	6.00	0.42	2.53	-24.29	-25.67	2.13	-4.65	0.84	0.16
72.7997° S	123	20	0.85	0.13	0.31	6.58	0.37	2.44	-23.57	-24.95	1.70	-5.08	0.73	0.47
group1	123	5	0.15	0.02	0.04	6.26	0.27	1.70	-23.88	-25.26	1.04	-5.74	0.56	0.97
	123	1	5.32	0.90		5.89			-26.27	-27.65	-0.43	-7.21	0.20	2.16
		total	7.91	1.34	0.90	5.90	0.35	2.06	-25.59		0.44		0.37	0.18
		bulk	8.25	1.49		5.52				1.38		6.78		22.17

Chemometric perspectives on plankton community responses to natural iron fertilization

T. W. Trull et al.

Title Page

Abstract

Introduction

Conclusions

References

Tables

Figures

◀

▶

◀

▶

Back

Close

Full Screen / Esc

Printer-friendly Version

Interactive Discussion



Table 2. Continued.

Station Date/location group	Volume L	fraction μm	POC μM	PN μM	PBSi μM	POC/PN atom	PBSi/POC atom	PBSi/PN atom	$\delta^{13}\text{CPOC}$ ‰ _{v-PDB}	$\delta^{13}\text{CPOC}-\delta^{13}\text{CDIC}$ ‰ _{v-PDB}	$\delta^{15}\text{NPN}$ ‰ _{air}	$\delta^{15}\text{NPN}-\delta^{15}\text{NO}_3$ ‰ _{air}	$\delta^{15}\text{NO}_3$ ‰ _{air}	f ratio	growth rate d^{-1} [CO_2] _{aq}
TEW 6	986	300	0.36	0.09	0.00	4.17	0.00	0.01	-23.24	-24.63	3.21	-3.61			
1 Nov 2011	986	210	0.12	0.03	0.00	4.47	0.03	0.12	-24.79	-26.18	2.98	-3.84			
48.4662° E	76	50	0.74	0.13	0.21	5.74	0.29	1.65	-23.59	-24.98	2.31	-4.51	0.87	0.18	
73.3998° S	76	20	0.77	0.12	0.31	6.51	0.40	2.63	-22.93	-24.32	2.10	-4.72	0.82	0.49	
group1	76	5	0.40	0.07	0.14	5.72	0.33	1.91	-23.42	-24.81	1.31	-5.51	0.62	1.00	
	76	1	6.91	1.33		5.20			-25.49	-26.88	0.19	-6.63	0.34	2.35	
		total	9.31	1.76	0.66	5.29	0.28	1.54	-24.94		0.71		0.43	0.20	
		bulk	6.38	1.14		5.62				1.39		6.82		22.17	
TEW 7	957	300	0.41	0.09	0.00	4.58	0.01	0.04	-22.23	-23.98	3.89	-3.87			
2 Nov 2011	957	210	0.13	0.03	0.00	4.97	0.02	0.09	-22.53	-24.28	3.65	-4.11			
48.4667° E	35	50	6.89	1.19	1.93	5.81	0.28	1.63	-20.48	-22.23	2.31	-5.45	0.64	0.20	
73.9992° S	35	20	2.32	0.37	0.81	6.27	0.35	2.20	-19.82	-21.57	2.38	-5.38	0.66	0.55	
group5	35	5	1.71	0.29	0.31	5.89	0.18	1.05	-21.38	-23.12	2.34	-5.42	0.64	1.03	
	35	1	8.43	1.58		5.32			-23.08	-24.83	2.08	-5.68	0.58	2.56	
		total	19.90	3.55	3.06	5.61	0.27	1.56	-21.63		2.27		0.61	0.22	
		bulk	22.82	4.09		5.58				1.75		7.76		20.04	
TEW 8	1509	300	0.13	0.03	0.00	4.90	0.01	0.05	-22.06	-23.80	3.79	-4.21			
2 Nov 2011	1509	210	0.04	0.01	0.00	5.04	0.10	0.48	-21.83	-23.57	3.81	-4.19			
48.4676° E	56	50	6.61	1.07	1.94	6.16	0.29	1.81	-20.53	-22.27	2.45	-5.55	0.61	0.17	
75.0032° S	56	20	7.10	1.15	1.65	6.17	0.23	1.43	-20.17	-21.91	2.60	-5.40	0.65	0.46	
group5	56	5	1.95	0.30	0.39	6.44	0.20	1.30	-21.14	-22.88	2.46	-5.54	0.61	0.91	
	56	1	9.02	1.73		5.23			-22.38	-24.12	1.95	-6.05	0.49	2.35	
		total	24.86	4.29	3.99	5.80	0.25	1.56	-21.16		2.30		0.57	0.19	
		bulk	23.21	3.92		5.92				1.74		8.00		17.43	
E 3	1246	300	0.07	0.01	0.00	4.84	0.04	0.20	-24.53	-25.94	3.47	-2.86			
4 Nov 2011	1246	210	0.03	0.01	0.01	5.25	0.31	1.65	-24.44	-25.85	3.05	-3.28			
48.6998° E	85	50	0.69	0.11	0.43	6.35	0.62	3.96	-23.64	-25.05	2.51	-3.82	1.04	0.17	
71.9670° S	85	20	1.25	0.19	0.68	6.68	0.55	3.64	-23.18	-24.59	2.09	-4.24	0.94	0.48	
group2	85	5	0.31	0.04	0.10	7.59	0.32	2.41	-23.92	-25.33	1.02	-5.31	0.67	0.95	
	85	1	6.79	1.24		5.48			-26.18	-27.59	-0.24	-6.57	0.36	2.14	
		total	9.13	1.60	1.22	5.72	0.52	3.43	-25.49		0.30		0.48	0.19	
		bulk	7.58	1.34		5.66				1.41		6.33		21.88	
F L	1102	300	0.13	0.02	0.01	5.46	0.06	0.32	-21.96	-23.60	3.38	-3.87			
6 Nov 2011	1102	210	0.19	0.04	0.03	4.98	0.17	0.87	-21.36	-23.00	3.11	-4.14			
48.5232° E	60	50	6.93	1.17	2.14	5.91	0.31	1.83	-20.85	-22.49	2.35	-4.90	0.78	0.17	
74.6673° S	60	20	5.32	0.92	1.42	5.80	0.27	1.55	-20.88	-22.52	2.33	-4.92	0.77	0.44	
group5	60	5	2.31	0.39	0.42	5.88	0.18	1.07	-21.44	-23.08	2.17	-5.08	0.73	0.90	
	60	1	7.51	1.41		5.32			-22.07	-23.71	2.14	-5.11	0.72	2.43	
		total	22.38	3.95	4.03	5.66	0.27	1.58	-21.34		2.26		0.75	0.18	
		bulk	15.76	2.89		5.45				1.64		7.25		17.43	
F S	571	300	0.23	0.05	0.02	5.03	0.10	0.52	-22.71	-24.42	3.50	-4.29			
8 Nov 2011	571	210	0.45	0.09	0.13	5.21	0.28	1.46	-22.34	-24.05	2.98	-4.81			
48.5006° E	110	50	13.05	2.20	4.80	5.93	0.37	2.18	-21.26	-22.97	2.61	-5.18	0.71	0.17	
73.9998° S	110	20	2.24	0.36	0.62	6.15	0.28	1.71	-21.32	-23.03	2.34	-5.45	0.64	0.45	
group5	110	5	1.34	0.23	0.27	5.91	0.20	1.21	-21.94	-23.66	2.22	-5.57	0.61	0.91	
	110	1	6.12	1.10		5.57			-22.51	-24.22	1.76	-6.03	0.49	2.48	
		total	23.43	4.02	5.85	5.82	0.34	2.00	-21.67		2.35		0.63	0.19	
		bulk	15.76	2.89		5.45				1.71		7.79		18.55	

Chemometric perspectives on plankton community responses to natural iron fertilization

T. W. Trull et al.

[Title Page](#)

[Abstract](#) [Introduction](#)

[Conclusions](#) [References](#)

[Tables](#) [Figures](#)

[◀](#) [▶](#)

[◀](#) [▶](#)

[Back](#) [Close](#)

[Full Screen / Esc](#)

[Printer-friendly Version](#)

[Interactive Discussion](#)



Table 2. Continued.

Station Date/location group	Volume L	fraction μm	POC μM	PN μM	PBSi μM	POC/PN atom	PBSi/POC atom	PBSi/PN atom	$\delta^{13}\text{CPOC}$ ‰ _{v-PDB}	$\delta^{13}\text{CPOC}-\delta^{13}\text{CDIC}$ ‰ _{v-PDB}	$\delta^{15}\text{NPN}$ ‰ _{air}	$\delta^{15}\text{NPN}-\delta^{15}\text{NO}_3$ ‰ _{air}	f ratio	growth rate d^{-1} [CO ₂] _{laq}
G 1	1457	300	0.11	0.02	0.05	5.69	0.44	2.53	-20.54	-22.09	3.84	-3.25		
8 Nov 2011	1457	210	0.25	0.04	0.13	5.78	0.52	2.99	-21.43	-22.99	2.10	-4.99		
49.9004° E	116	50	13.92	2.20	11.04	6.32	0.79	5.01	-21.43	-22.99	1.24	-5.85	0.54	0.20
71.8991° S	116	20	0.50	0.08	0.32	6.58	0.65	4.25	-20.44	-22.00	0.94	-6.15	0.46	0.57
group3	116	5	0.38	0.06	0.23	6.29	0.61	3.81	-21.25	-22.81	0.39	-6.70	0.32	1.14
	116	1	3.64	0.73		5.00			-22.25	-23.80	1.85	-5.24	0.69	3.01
		total	18.79	3.13	11.77	6.01	0.78	4.90	-21.56		1.38		0.57	0.22
		bulk	19.40	3.29	5.90					1.55		7.09		21.59
G 2	631	300	0.03	0.01	0.00	5.78	0.06	0.36	-22.64	-24.19	4.41	-2.12		
9 Nov 2011	631	210	0.16	0.03	0.08	5.52	0.50	2.77	-18.04	-19.60	3.61	-2.92		
49.1331° E	61	50	1.94	0.32	1.07	6.03	0.55	3.34	-18.16	-19.71	3.34	-3.19	1.20	0.22
70.6498° S	61	20	3.63	0.61	1.21	5.93	0.33	1.98	-18.99	-20.54	2.96	-3.57	1.11	0.56
group4	61	5	0.92	0.17	0.21	5.54	0.23	1.25	-21.40	-22.95	2.84	-3.69	1.08	1.01
	61	1	5.97	1.12		5.33			-20.82	-22.37	3.88	-2.65	1.34	2.99
		total	12.66	2.25	2.57	5.61	0.39	2.27	-19.90		3.47		1.23	0.24
		bulk	13.10	2.35	5.56					1.55		6.53		19.25
E 4W	393	300	0.07	0.01	0.02	6.38	0.33	2.09	-23.73	-25.13	2.81	-3.58		
11 Nov 2011	393	210	0.05	0.01	0.01	6.36	0.26	1.65	-24.20	-25.60	3.44	-2.95		
48.7667° E	43	50	7.09	1.23	4.53	5.77	0.64	3.69	-22.29	-23.69	1.41	-4.98	0.75	0.18
71.4294° S	43	20	1.18	0.18	0.67	6.55	0.57	3.70	-22.01	-23.41	1.09	-5.30	0.68	0.50
group3	43	5	0.43	0.06	0.18	7.46	0.43	3.21	-22.80	-24.20	0.28	-6.11	0.47	0.99
	43	1	6.32	1.31		4.83			-23.61	-25.01	1.41	-4.98	0.76	2.63
		total	15.14	2.79	5.42	5.42	0.61	3.65	-22.85		1.38		0.74	0.20
		bulk	12.58	2.18	5.78					1.40		6.39		20.73
E 4E	974	300	0.14	0.03	0.02	4.80	0.12	0.58	-23.17	-24.69	3.13	-3.49		
13 Nov 2011	974	210	0.24	0.05	0.06	4.71	0.26	1.23	-23.19	-24.71	3.44	-3.18		
48.7141° E	32	50	3.12	0.54	1.74	5.74	0.56	3.20	-22.71	-24.24	2.46	-4.16	0.96	0.17
72.5708° S	32	20	1.86	0.29	1.12	6.39	0.61	3.87	-22.23	-23.75	1.82	-4.80	0.80	0.48
group2	32	5	0.80	0.13	0.33	6.29	0.42	2.62	-23.21	-24.73	0.80	-5.82	0.54	0.94
	32	1	11.19	2.01		5.55			-23.20	-24.72	1.35	-5.27	0.68	2.48
		total	17.35	3.06	3.28	5.68	0.53	3.15	-23.01		1.62		0.74	0.19
		bulk	9.90	1.70	5.83					1.53		6.62		20.63
A3 2 night	586	300	0.04	0.01	0.01	4.83	0.17	0.80	-22.85	-24.16	3.79	-2.53		
15 Nov 2011	586	210	0.05	0.01	0.01	4.80	0.18	0.85	-24.43	-25.74	4.02	-2.30		
50.6300° E	161	50	6.42	1.06	4.65	6.08	0.72	4.40	-21.86	-23.17	1.06	-5.26	0.69	0.19
72.0802° S	161	20	0.30	0.05	0.19	6.03	0.64	3.89	-22.19	-23.50	0.62	-5.70	0.58	0.51
group3	161	5	0.09	0.02	0.08	5.81	0.92	5.37	-22.34	-23.66	0.62	-5.70	0.57	1.06
	161	1	1.84	0.38		4.87			-22.14	-23.46	1.55	-4.77	0.81	3.04
		total	8.74	1.52	4.94	5.76	0.72	4.33	-21.95		1.20		0.71	0.21
		bulk	9.60	1.78	5.38					1.31		6.32		21.04
A3 2 day	1081	300	0.06	0.01	0.00	5.26	0.08	0.43	-22.78	-24.12	4.02	-2.47		
16 Nov 2011	1081	210	0.12	0.02	0.04	5.48	0.34	1.86	-22.30	-23.64	2.81	-3.68		
50.6300° E	209	50	6.36	0.96	4.66	6.63	0.73	4.86	-21.83	-23.16	1.54	-4.95	0.76	0.19
72.0802° S	209	20	0.34	0.05	0.24	6.47	0.70	4.53	-20.91	-22.24	0.69	-5.80	0.55	0.55
group3	209	5	0.14	0.02	0.09	6.11	0.64	3.89	-21.67	-23.01	0.05	-6.44	0.39	1.10
	209	1	2.90	0.58		5.03			-21.95	-23.28	1.45	-5.04	0.74	3.07
		total	9.91	1.64	5.03	6.03	0.72	4.72	-21.84		1.49		0.74	0.22
		bulk	13.06	2.28	5.72					1.33		6.49		20.96

Chemometric perspectives on plankton community responses to natural iron fertilization

T. W. Trull et al.

Title Page

Abstract Introduction

Conclusions References

Tables Figures

◀ ▶

◀ ▶

Back Close

Full Screen / Esc

Printer-friendly Version

Interactive Discussion



Chemometric perspectives on plankton community responses to natural iron fertilization

T. W. Trull et al.

Table 2. Continued.

Station Date/location group	Volume L	fraction μm	POC μM	PN μM	PBSi μM	POC/PN atom	PBSi/POC atom	PBSi/PN atom	$\delta^{13}\text{CPOC}$ ‰ _{vs-PDB}	$\delta^{13}\text{CPOC}-\delta^{13}\text{CDIC}$ ‰ _{vs-PDB}	$\delta^{15}\text{NPN}$ ‰ _{air}	$\delta^{15}\text{NPN}-\delta^{15}\text{NO}_3$ ‰ _{air}	f ratio	growth rate d^{-1} $[\text{CO}_2]_{\text{aq}}$
E 4W 2	1373	300	0.14	0.03	0.04	4.49	0.28	1.27	-24.25	-25.74	2.57	-3.98		
18 Nov 2011	1373	210	0.71	0.13	0.40	5.36	0.57	3.03	-23.93	-25.42	2.08	-4.47		
48.7666° E	131	50	6.82	1.13	6.42	6.02	0.94	5.66	-23.22	-24.71	1.82	-4.73	0.82	0.17
71.4798° S	131	20	0.24	0.04	0.17	6.27	0.71	4.44	-22.77	-24.26	1.35	-5.20	0.70	0.47
group3	131	5	0.27	0.05	0.13	5.62	0.50	2.79	-22.50	-23.99	-0.23	-6.78	0.31	1.02
	131	1	3.97	0.72		5.54			-25.00	-26.50	0.38	-6.17	0.46	2.33
		total	12.15	2.10	7.16	5.78	0.88	5.18	-23.83		1.30		0.67	0.19
		bulk	13.36	2.51	5.32					1.49		6.55		20.96
E 5	992	300	0.29	0.07	0.01	4.02	0.05	0.20	-23.96	-25.40	2.97	-3.64		
18 Nov 2011	992	210	0.11	0.03	0.01	4.43	0.13	0.57	-25.14	-26.58	2.94	-3.67		
48.4178° E	195	50	2.08	0.36	1.31	5.84	0.63	3.67	-24.42	-25.86	1.74	-4.87	0.78	0.16
71.9973° S	195	20	0.44	0.07	0.28	6.53	0.63	4.11	-23.38	-24.82	1.40	-5.21	0.70	0.46
group2	195	5	0.16	0.03	0.07	6.14	0.44	2.70	-23.21	-24.65	-0.14	-6.75	0.31	0.98
	195	1	2.60	0.46		5.61			-25.72	-27.16	-0.99	-7.60	0.10	2.19
		total	5.67	1.01	1.68	5.62	0.55	3.08	-24.90		0.53		0.42	0.18
		bulk	7.59	1.31	5.78					1.44		6.61		21.43

Bolded column headers refer to bolded quantities shown on the bulk sample lines; bulk samples were measured on water and unfractionated particle samples collected separately.

Title Page

Abstract

Introduction

Conclusions

References

Tables

Figures



Back

Close

Full Screen / Esc

Printer-friendly Version

Interactive Discussion



Chemometric perspectives on plankton community responses to natural iron fertilization

T. W. Trull et al.

[Title Page](#)

[Abstract](#)

[Introduction](#)

[Conclusions](#)

[References](#)

[Tables](#)

[Figures](#)

[◀](#)

[▶](#)

[◀](#)

[▶](#)

[Back](#)

[Close](#)

[Full Screen / Esc](#)

[Printer-friendly Version](#)

[Interactive Discussion](#)



Table 3. Phytoplankton cell dimensions used in ^{13}C supply vs. demand model.

Size Fraction μm	Prism Dimensions			Form
	d1	d2	d3	
1–5	3	3	3	single cells
5–20	7	7	15	single cells
20–50	15	15	30	chains*
50–210	40	40	80	chains*

* CO_2 exchange is assumed to be negligible on the surface of the cell contact within the chains, taken to be the long faces of the prisms.

Chemometric perspectives on plankton community responses to natural iron fertilization

T. W. Trull et al.

Title Page

Abstract

Introduction

Conclusions

References

Tables

Figures

⏪

⏩

◀

▶

Back

Close

Full Screen / Esc

Printer-friendly Version

Interactive Discussion

Table 4. Surface mixed layer nutrient depletion and export estimates.

Station	CTD	timestamp cast mm-dd hh-mm	Depth MLD ¹ m	T_{\min} m	$S_{\text{threshold}}$ m	Nitrate surface μM	T_{\min} μM	$S_{\text{threshold}}$ μM	Nitrate depletion		PN stock 200 m mmol m^{-2}	N Export ² $S_{\text{threshold}}$ mmol m^{-2}	N Export ³ fraction %
									T_{\min} mmol m^{-2}	$S_{\text{threshold}}$ mmol m^{-2}			
A3-1	4	10-20 05:32	161	175	175	29.1	31.1	31.1	268	268	138	130	49
TNS10	6	10-21 07:28	163	183	179	28.9	31.1	31.0	298	270	193	77	28
TNS09	7	10-21 13:40	137	147	150	27.9	30.3	30.7	243	324	205	119	37
TNS08	8	10-21 18:48	139	192	201	27.9	30.8	31.2	362	470	179	291	62
TNS06	10	10-22 11:18	67	280 ⁴	149	26.5	33.5	29.8	1034	317	219	99	31
TNS05	11	10-22 16:56	114	174 ⁴	155	26.5	30.1	29.5	438	345	164	181	52
TNS03	13	10-23 06:41	111	191 ⁴	164	26.9	31.0	29.9	494	326	144	183	56
TNS02	14	10-23 12:06	65	364 ⁴	150	19.5	34.0	28.8	1711	279	101	179	64
TNS01	15	10-23 17:13	45	328 ⁴	144	23.6	31.2	25.5	1506	196	135	61	31
R2	17	10-25 22:59	111	184 ⁴	168	25.7	28.0	27.3	346	232	78	154	66
R2	18	10-26 01:48	123	193	167	26.0	28.3	27.3	430	239	78	161	67
E-1	27	10-29 22:46	84	200	173	25.7	29.0	28.6	492	421	208	213	51
E-1	30	10-30 09:15	63	183	151	26.0	29.0	30.8	293	493	208	285	58
TEW3	38	10-31 18:41	62	165 ⁴	138	27.2	29.1	28.1	225	89	145	-56	-63
TEW4	42	11-01 05:19	95	208	185	25.0	30.1	29.2	631	463	250	213	46
TEW5	44	11-01 19:00	60	173	174	26.1	30.2	29.8	434	354	201	153	43
TEW6	45	11-02 03:59	22	164	142	26.0	30.9	30.1	493	371	175	197	53
TEW7	46	11-02 09:34	17	423 ⁴	91	26.0	35.0	27.0	2103	391	309	82	21
TEW8	47	11-02 18:47	22	293 ⁴	75	19.5	32.7	27.2	1282	303	252	51	17
E-2	43	11-01 12:00	42	210 ⁴	157	18.9	32.7	29.3	857	221	185	36	16
E-3	50	11-03 11:57	41	203	177	25.4	30.1	29.5	467	371	194	177	48
E-3	51	11-04 01:29	32	200	166	25.8	30.0	28.7	486	253	194	59	23
E-3	55	11-04 17:22	37	184	161	26.0	29.5	28.6	520	361	194	166	46
F-L	63	11-06 21:49	21	182	79	26.0	30.5	26.4	686	368	215	153	42
F-S	69	11-08 06:13	31	267	54	18.9	35.2	24.7	1598	140	354	-214	-153
G-1	70	11-09 00:30	37	118	127	19.9	29.8	30.3	380	447			
E-4W	79	11-11 08:25	67	158	147	23.0	30.2	30.1	548	527	288	239	45
E-4W	81	11-11 21:07	67	152	158	22.1	30.1	30.0	544	532	288	243	46
E-4W	87	11-12 09:30	66	164	164	22.1	30.4	30.3	652	645	288	357	55
E-4E	94	11-13 22:02	77	158	108	22.1	28.8	27.7	382	236	253	-17	-7
E-4E	95	11-14 01:30	80	159	112	24.1	28.9	27.4	439	227	253	-26	-11
A3-2	99	11-15 23:20	143	179	179	24.1	30.6	30.7	652	670	436	234	35
A3-2	108	11-17 01:08	123	182	177	25.8	30.9	30.8	593	576	436	140	24
E_4W-2	111	11-18 07:20	26	168	133	24.7	29.3	28.0	592	400	354	46	11
E-5	113	11-18 19:21	71	215	122	26.5	30.4	27.9	689	207	210	-3	-1
E-5	114	11-18 22:07	36	228	126	26.5	30.8	28.0	756	206	210	-4	-2
E-5	115	11-19 01:30	41	222 ⁴	123	26.5	30.7	27.9	686	222	210	12	6

Chemometric perspectives on plankton community responses to natural iron fertilization

T. W. Trull et al.

Title Page

Abstract

Introduction

Conclusions

References

Tables

Figures

◀

▶

◀

▶

Back

Close

Full Screen / Esc

Printer-friendly Version

Interactive Discussion

Table 4. Continued.

Station	CTD	timestamp	Depth MLD ¹ m	Silicate			Silicate Depletion		BSi Stock 200 m mmol m ⁻²	Si Export ² mmol m ⁻²	Si Export ³ fraction %		
				T_{min} m	$S_{threshold}$ m	surface μM	T_{min} μM	$S_{threshold}$ μM				T_{min} mmol m ⁻²	$S_{threshold}$ mmol m ⁻²
A3-1	4	10-20 05:32	161	175	175	10.79	27.12	27.12	551	551	163.5	388	70
TNS10	6	10-21 07:28	163	183	179	23.27	30.58	29.71	1244	1086	284.5	802	74
TNS09	7	10-21 13:40	137	147	150	18.74	25.27	27.07	838	1105	499.1	606	55
TNS08	8	10-21 18:48	139	192	201	17.03	22.92	23.70	884	1154	364.8	789	68
TNS06	10	10-22 11:18	67	280 ⁴	149	16.42	48.25	26.18	5896	1170	257.3	913	78
TNS05	11	10-22 16:56	114	174 ⁴	155	16.98	27.82	23.48	1529	811	239.9	571	70
TNS03	13	10-23 06:41	111	191 ⁴	164	19.32	32.79	25.54	2092	806	209.3	597	74
TNS02	14	10-23 12:06	65	364 ⁴	150	15.27	48.41	18.39	8116	307	127.9	179	58
TNS01	15	10-23 17:13	45	328 ⁴	144	7.48	33.92	10.15	5875	243	33.5	210	86
R2	17	10-25 22:59	111	184 ⁴	168	12.07	19.54	17.11	1145	718	88.6	630	88
R2	18	10-26 01:48	123	193	167	12.34	19.28	17.25	1001	634	88.6	546	86
E-1	27	10-29 22:46	84	200	173	14.94	30.42	25.24	2426	1467	332.6	1134	77
E-1	30	10-30 09:15	63	183	151	16.29	36.63	29.30	2794	1571	332.6	1238	79
TEW3	38	10-31 18:41	62	165 ⁴	138	18.63	26.52	24.23	893	547	141.0	406	74
TEW4	42	11-01 05:19	95	208	185	14.13	27.73	23.86	2128	1359	460.3	898	66
TEW5	44	11-01 19:00	60	173	174	14.47	24.81	24.99	1245	1276	145.0	1131	89
TEW6	45	11-02 03:59	22	164	142	15.83	28.41	23.92	1615	923	213.8	709	77
TEW7	46	11-02 09:34	17	423 ⁴	91	5.91	50.03	15.85	10392	557	326.2	230	41
TEW8	47	11-02 18:47	22	293 ⁴	75	6.19	36.81	16.72	4532	433	250.4	183	42
E-2	43	11-01 12:00	42	210 ⁴	157	14.52	38.83	22.79	3729	799	306.7	492	62
E-3	50	11-03 11:57	41	203	177	15.10	28.92	24.10	2033	1117	285.5	832	74
E-3	51	11-04 01:29	32	200	166	15.04	25.77	22.49	1433	833	285.5	548	66
E-3	55	11-04 17:22	37	184	161	14.81	29.39	25.69	1978	1340	285.5	1055	79
F-L	63	11-06 21:49	21	182	79	7.23	24.32	13.74	1688	373	313.8	59	16
F-S	69	11-08 06:13	31	267	54	9.88	39.60	13.42	4470	116	377.6	-261	-225
G-1	70	11-09 00:30	37	118	127	9.61	23.99	26.12	968	1228			
E-4W	79	11-11 08:25	67	158	147	17.47	29.18	26.67	1255	870	379.5	490	56
E-4W	81	11-11 21:07	67	152	158	17.95	23.89	25.53	433	689	379.5	309	45
E-4W	87	11-12 09:30	66	164	164	17.00	26.26	26.26	1002	1002	379.5	622	62
E-4E	94	11-13 22:02	77	158	108	12.10	22.79	18.95	1034	520	427.0	92	18
E-4E	95	11-14 01:30	80	159	112	11.60	20.87	17.45	999	519	427.0	92	18
A3-2	99	11-15 23:20	143	179	179	19.82	27.32	27.32	1091	1091	713.3	378	35
A3-2	108	11-17 01:08	123	182	177	18.60	28.60	28.16	1231	1151	713.3	438	38
E-4W-2	111	11-18 07:20	26	168	133	9.21	30.44	22.24	2532	1297	744.3	552	43
E-5	113	11-18 19:21	71	215	122	12.04	30.72	16.98	2801	484	744.3	-260	-54
E-5	114	11-18 22:07	36	228	126	11.53	31.35	19.45	3139	707	744.3	-37	-5
E-5	115	11-19 01:30	41	222 ⁴	123	11.49	26.00	19.22	1873	704	394.4	310	44

¹ Mixed layer depth where the potential density = potential density at 10 m + 0.02 kg m⁻³. Park et al. (2014b).

² Fraction = export/depletion, calculated for the $S_{threshold}$ depletion estimate.

³ Percent depletion of the winter mixed layer inventory.

⁴ No clear T_{min} .

Surface data are from both the CTD Niskin bottles and underway systems. T_{min} nitrate was estimated from nearest Niskin.

Chemometric perspectives on plankton community responses to natural iron fertilization

T. W. Trull et al.

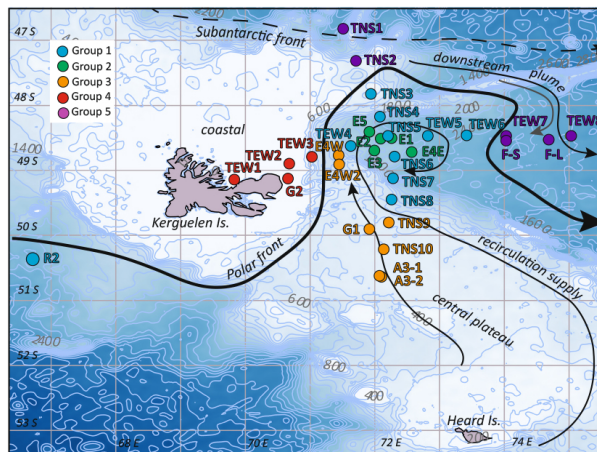


Figure 1. Map of KEOPS-2 station locations. The Kerguelen and Heard islands mark the northern and southern end of the central plateau (bathymetry in meters). The Polar Front jet that passes through the mid-depth channel south of Kerguelen Island is shown as a bold line. Full ocean depth flows of the Antarctic Circumpolar Current pass to the north of Kerguelen Island in association with the Subantarctic Front and to the south of Heard Island in the Fawn Trough. This latter flow follows the eastern slope of the plateau northwards to bring cold waters into a bathymetrically trapped quasi-stationary recirculation feature (d’Ovidio et al., 2014; Park et al., 2014b). Waters over the central plateau are also carried into this region. During the initial survey, the TNS transect was sampled first (south to north) and then the TEW transect (west to east). The E stations were designed to provide a Lagrangian temporal sequence in the recirculation region (including some to the east and west of its centre), with interspersed visits to the HNLC reference station (R2); the region of high biomass near and north of the Polar Front (F-L and F-S), and the central plateau bloom station (A3) previously studied in autumn 2005 by the KEOPS project. Two additional stations (G1, G2) carried out for high volume geochemical tracer studies and provided additional plateau and coastal samples, respectively. The stations are colour coded into 5 Groups as shown on the map (QGIS) and detailed in Table 1.

Title Page

Abstract

Introduction

Conclusions

References

Tables

Figures

◀

▶

◀

▶

Back

Close

Full Screen / Esc

Printer-friendly Version

Interactive Discussion

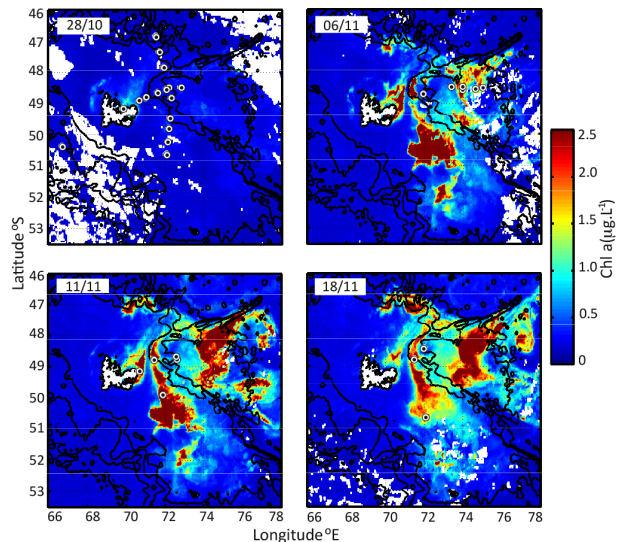


Figure 2. Temporal development of the Kerguelen bloom. Successive images of surface chlorophyll distributions (NASA MODIS-Aqua; SSALTO/DUACS 1 km daily product) show the bloom development. Image date 28 October: most stations of the initial survey downstream of Kerguelen Island (TNS 1–10, TEW 1–6), the HNLC reference station (R2, upstream) and the first visit to the KEOSP1 plateau reference station (A3–1 at the southern end of the TNS transect) were sampled before any significant biomass accumulation had occurred. Image date 6 November: the developing downstream Polar Front bloom (TEW 7, TEW 8, F-L, F-S) was sampled early in its development, and the recirculation visited a second time (E2). Image date 11 November: the now well developed central plateau bloom was sampled (G1; E4-W) along with also blooming coastal waters (G2). Two more visits to the still low biomass recirculation were also completed (E3 and E4-E). Image date 18 November: the plateau bloom was re-sampled as it began to fade (A3–2 and E4-W2), along with the final recirculation station (E5). Bathymetry is shown by contours at 1000, 200, and 300 m depths. A full annual animation of the phytoplankton bloom evolution is available in the supplementary materials.

Chemometric perspectives on plankton community responses to natural iron fertilization

T. W. Trull et al.

Title Page

Abstract

Introduction

Conclusions

References

Tables

Figures

◀

▶

◀

▶

Back

Close

Full Screen / Esc

Printer-friendly Version

Interactive Discussion



Chemometric perspectives on plankton community responses to natural iron fertilization

T. W. Trull et al.

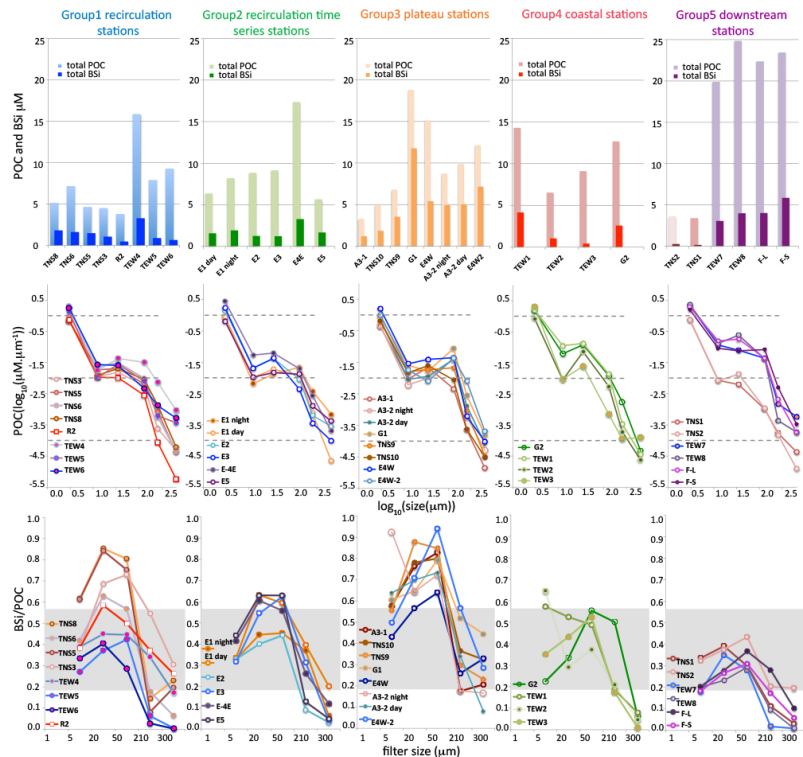


Figure 3. Surface water total and size-fractionated POC and BSi concentrations. Top row: total POC and BSi concentrations for the identified station Groups (see Table 1); individual stations in each group are in chronological order from left to right. Middle row: POC size distribution spectra, i.e. concentrations normalised by dividing by the width of the size fraction (i.e. division by 4 for the 1–5 μm fraction); dotted lines provide visual guides and reveal little variation among groups for the smallest particles, and largest variations in the intermediate size fractions. Bottom row: BSi/POC ratios; grey band indicates approximate range of values for extant diatoms, with higher values possibly indicative of higher iron stress.

Title Page

Abstract

Introduction

Conclusions

References

Tables

Figures



Back

Close

Full Screen / Esc

Printer-friendly Version

Interactive Discussion

Chemometric perspectives on plankton community responses to natural iron fertilization

T. W. Trull et al.

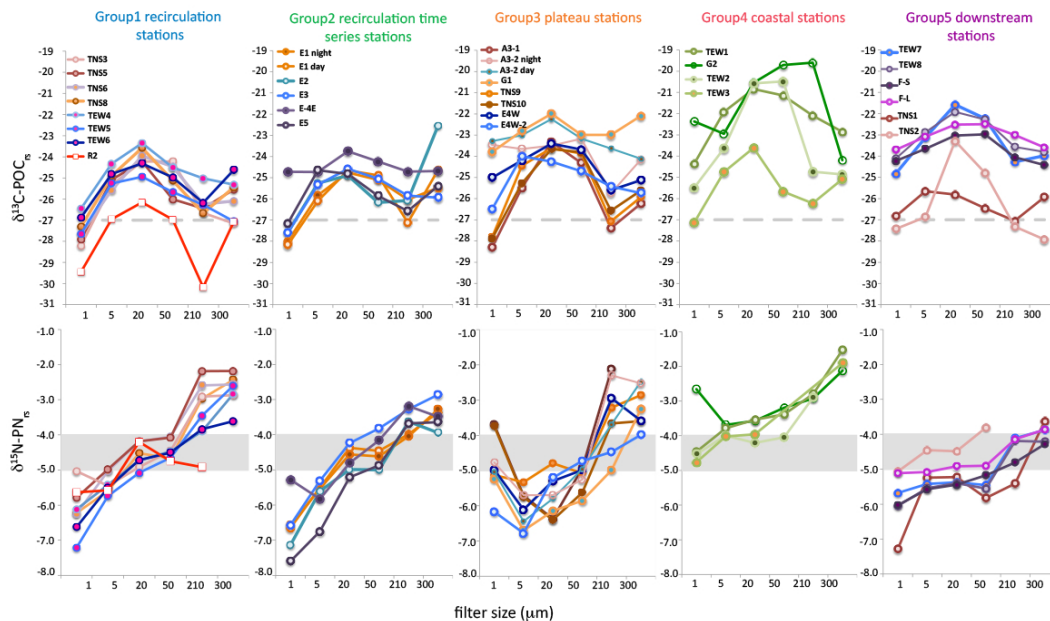


Figure 4. Isotopic variations in the size-fractionated particles. Top row: ^{13}C -POC values relative to ^{13}C -DIC values; dotted line shows the lowest values for the intermediate, autotrophic, size fractions samples as observed at upstream Fe poor reference station (R2). Bottom row: ^{15}N -PON values relative to co-located ^{15}N - NO_3^- values; grey band indicates values expected for phytoplankton that grow exclusively on nitrate.

Chemometric perspectives on plankton community responses to natural iron fertilization

T. W. Trull et al.

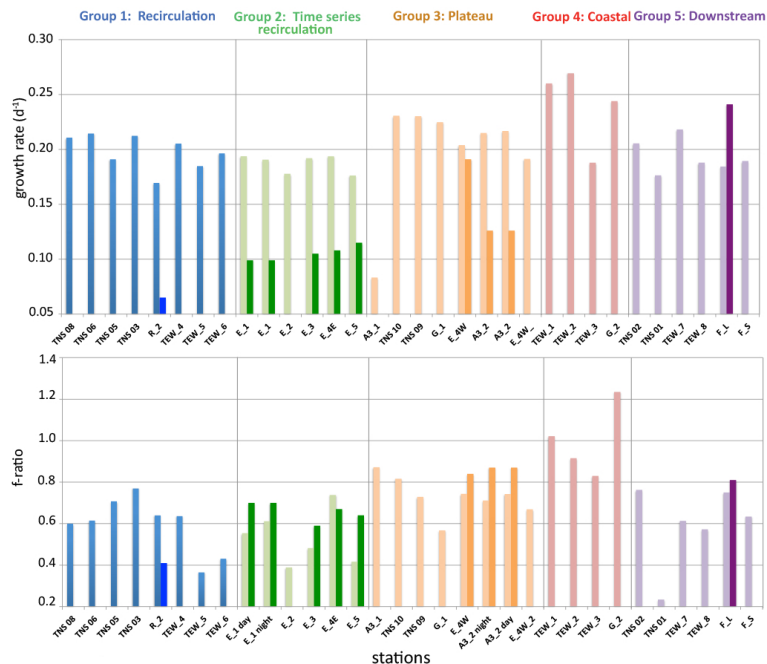


Figure 5. Isotopic chemometric estimates of growth rates and f ratios. Top row: growth rates based on the supply vs. demand ^{13}C isotopic fractionation model (summed across the 4 smallest particle size fractions). Estimates from a limited set of ^{13}C tracer uptake incubations are shown as darker bars (measured at varying light levels and integrated to the mixed layer depth light level; Cavagna et al., 2014). Bottom row: f ratios, i.e. the fraction of total nitrogen nutrition provided by nitrate, based on the ^{15}N ammonium and ^{15}N nitrate end-member mixing model (summed across 4 smallest particle size fractions). Estimates from a limited set of ^{15}N tracer uptake incubations are shown as darker bars (Cavagna et al., 2014).

Title Page

Abstract

Introduction

Conclusions

References

Tables

Figures

◀

▶

◀

▶

Back

Close

Full Screen / Esc

Printer-friendly Version

Interactive Discussion

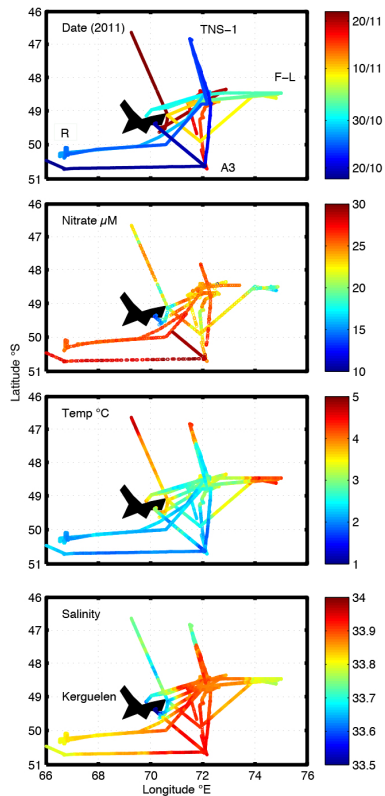


Figure 6. High resolution distributions of surface water properties from continuous sensor measurements. Top to bottom: ship trajectory as revealed by dates of sampling; nitrate concentrations (from UV spectrometry, temperature, and salinity, ISUS). Stations at the ends of the trajectories are indicated to aid in co-location with the lower resolution station sampling map (Fig. 1).

Chemometric perspectives on plankton community responses to natural iron fertilization

T. W. Trull et al.

Title Page

Abstract Introduction

Conclusions References

Tables Figures

◀ ▶

◀ ▶

Back Close

Full Screen / Esc

Printer-friendly Version

Interactive Discussion



Chemometric perspectives on plankton community responses to natural iron fertilization

T. W. Trull et al.

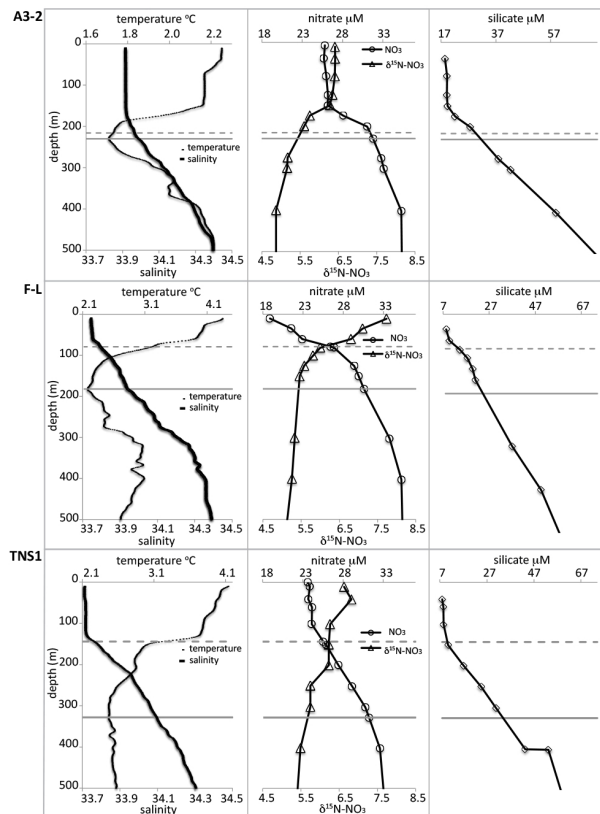


Figure 7. Example profiles of temperature, salinity, nitrate concentrations, and nitrate isotopic compositions. Top row: group 3 central plateau station A3-2. Middle row: group 5 downstream Polar Front station F-L. Bottom row: group 5 Subantarctic station TNS-1. Depths of the remnant winter water T_{\min} mixed layer depth (T_{\min} -depth; solid line) and salinity stratification mixed layer depth ($S_{\text{threshold}}$ -depth; dotted lines) are shown. These depths define our two approaches for the calculation of depth integrated nitrate and silicate depletions (Table 4; Fig. 8).

Title Page

Abstract

Introduction

Conclusions

References

Tables

Figures

◀

▶

◀

▶

Back

Close

Full Screen / Esc

Printer-friendly Version

Interactive Discussion

Chemometric perspectives on plankton community responses to natural iron fertilization

T. W. Trull et al.

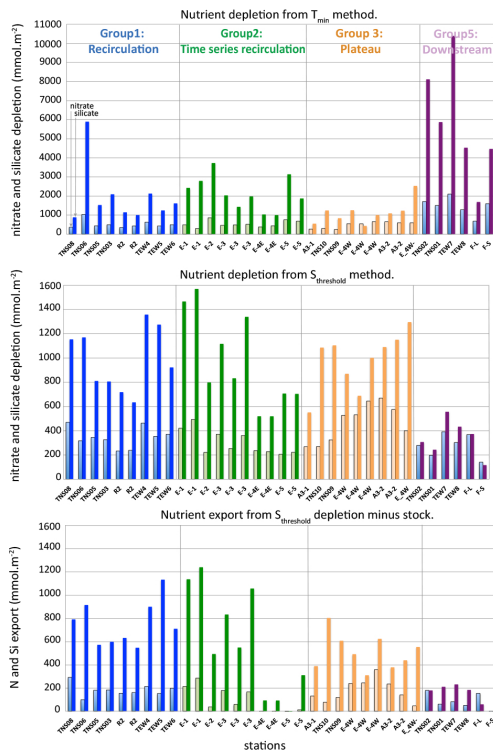


Figure 8. Nitrogen and silicon depletion and export estimates. Top row: nitrate (light bars) and silicate (dark bars) depletions from the T_{\min} winter concentration method. Middle row: nitrate (light bars) and silicate (dark bars) depletions from the $S_{\text{threshold}}$ winter concentration method. Bottom row: N (light bars) and Si (dark bars) export, as estimated from the $S_{\text{threshold}}$ depletion method, after accounting for the PN and BSi standing stocks integrated to 200 m (Table 4; Lasbleiz et al., 2014). Group 4 coastal stations are not shown because CTD casts could not define winter values. Negative export values are not plotted. Groups 1, 2, 3 and 4 are coloured as in Fig. 1 and are ranked from left to right with temporal order within each group.